

RESEARCH ARTICLE

Dietary resistant starch preserved through mild extrusion of grain alters fecal microbiome metabolism of dietary macronutrients while increasing immunoglobulin A in the cat

Matthew I. Jackson¹*, Christopher Waldy, Dennis E. Jewell²

Pet Nutrition Center, Hill's Pet Nutrition, Inc., Topeka, KS, United States of America

✉ Current address: Kansas State University, Manhattan, Kansas, United States of America

* matthew_jackson@hillspet.com**OPEN ACCESS**

Citation: Jackson MI, Waldy C, Jewell DE (2020) Dietary resistant starch preserved through mild extrusion of grain alters fecal microbiome metabolism of dietary macronutrients while increasing immunoglobulin A in the cat. PLoS ONE 15(11): e0241037. <https://doi.org/10.1371/journal.pone.0241037>

Editor: Juan J. Loor, University of Illinois, UNITED STATES

Received: November 25, 2019

Accepted: October 7, 2020

Published: November 3, 2020

Copyright: © 2020 Jackson et al. This is an open access article distributed under the terms of the [Creative Commons Attribution License](https://creativecommons.org/licenses/by/4.0/), which permits unrestricted use, distribution, and reproduction in any medium, provided the original author and source are credited.

Data Availability Statement: Sequences were deposited in the NCBI Sequence Read Archive under accession number PRJNA63518. All other data are available in the paper and its [Supporting Information](#) files.

Funding: Hill's Pet Nutrition provided funding for this study in the form of salaries for MJJ, CW, and DEJ. The specific roles of these authors are articulated in the 'author contributions' section. The funder was given the opportunity to read the

Abstract

Dietary digestion-resistant starch (RS) provides health benefits to the host via gut microbiome-mediated metabolism. The degree to which cats manifest beneficial changes in response to RS intake was examined. Healthy cats (N = 36) were fed identically formulated foods processed under high (n = 17) or low (n = 19) shear extrusion conditions (low and high RS levels [LRS and HRS], respectively). Fecal samples collected after 3 and 6 weeks' feeding were assayed for stool firmness score, short-chain fatty acids, ammonia, and changes to the global metabolome and microbiome; fecal immunoglobulin A (IgA) was analyzed at week 6. Few differences were seen in proximate analyses of the foods; stool firmness scores did not differ. In cats consuming HRS food, concentrations of fecal butyrate and the straight chain:branched chain fatty acid ratio were significantly greater in feces at both weeks 3 and 6, while fecal ammonia was reduced at week 6 relative to feces from LRS-fed cats. Fecal IgA concentrations were significantly higher at week 6 with HRS food. RS consumption altered 47% of the fecal metabolome; RS-derived sugars and metabolites associated with greater gut health, including indoles and polyamines, increased in the cats consuming HRS food relative to those fed the LS food, while endocannabinoid N-acyl ethanolamines decreased. Consumption of HRS food increased concentrations of the ketone body 3-hydroxybutyrate in feces and elevated concentrations of reduced members of NADH-coupled redox congeners and NADH precursors. At the microbiome genus-level, 21% of operational taxonomic units were significantly different between food types; many involved taxa with known saccharolytic or proteolytic proclivities. Microbiome taxa richness and Shannon and Simpson alpha diversity were significantly higher in the HRS group at both weeks. These data show that feline consumption of grain-derived RS produces potentially beneficial shifts in microbiota-mediated metabolism and increases IgA production.

manuscript prior to publication, but played no further role in study design, data collection and analysis, decision to publish, or preparation of the manuscript.

Competing interests: The authors have read the journal's policy and have the following competing interests: MJ and CW are current employees of Hill's Pet Nutrition, and DEJ is a former employee of Hill's Pet Nutrition, which provided funding for this study. The authors would like to declare the following patent applications associated with this research: "Pet food composition and method of making pet food composition comprising enhanced levels of resistant starch" (WO2019112562A1). This does not alter our adherence to PLOS ONE policies on sharing data and materials.

Introduction

The lower gut of monogastric animals harbors communities of microbiota (ie, the microbiome). In this mutualistic relationship, dietary nutrients escaping host digestion and absorption become available to the microbiome while the microbiome concomitantly generates a number of small molecule metabolites (postbiotics) that act locally in the gastrointestinal tract and are also reabsorbed across the colon to systemic circulation [1]. Microbiome function and production of postbiotics have a large impact on host health, so characterization of these metabolites can provide insights into optimal health [2, 3]. Food processing through extrusion can increase the digestibility and bioavailability of nutrients to the host while restricting their access to the colonic microbiota. During extrusion, the ingredients are cooked using both mechanical shear force and heat; each of these parameters can be scaled on a spectrum from mild to intense. Depending on conditions, extrusion can improve the digestibility of protein [4] and amino acids [5] and increase fiber-carbohydrate solubility by degrading plant cell walls [6]. Most foods destined for consumption by companion animals are extruded and the consequences for pet nutrition have been reviewed [7]. Grains are prominent sources of dietary starch and serve as a source of energy, fiber, and protein for companion animals and also enable formation of a dry, extruded pet food kibble with appropriate expansion.

Nutrient digestibility is typically paramount in food production, and extrusion aids in achieving this goal. Recently however, mild conditions of grain extrusion with reduced mechanical shear force and heat have been utilized to retain type 2 ungelatinized dietary digestion-resistant starch (RS) [8]. Additionally, decreased shear force reduces scission of high molecular weight starch [9]; both RS and high molecular weight starch polymers are less digestible and thus arrive relatively intact to the large intestine.

Increasing RS through mild food processing can provide health benefits via the intermediary of the action of gut microbes to ferment RS to beneficial catabolic products, as has been observed for humans [10] and dogs [11]. Varying the conditions of grain extrusion has been shown to modify microbiome composition *in vitro* as well as the degree to which microbiota produce fermentation products [12]. Domesticated felines (*Felis catus*) are obligate carnivores; however, RS consumption might be expected to influence their microbiome composition and activity since phylogeny and functional gene content of the domesticated cat microbiome is similar to that of omnivores [13] and also markedly different from that of both captive and non-captive wild felines [14]. Although there are reports examining the effects of non-starch polysaccharide fibers added to diets of cats [15–18], there are no published reports of the microbiome effects of dietary intervention in cats with foods designed to vary in RS concentrations.

The metabolic functions of the microbiome that act on dietary constituents can roughly be classified as saccharolytic, proteolytic, and lipolytic. The microbiome can carry out the saccharolysis of intact starch granules in the colon to produce fermentative postbiotics including short-chain fatty acids (SCFA) [19], which have a number of beneficial physiological effects [20]. Dietary protein escaping digestion can be subjected to proteolysis by the microbiome and the resultant amino acids putrefied to products, including branched-chain fatty acids (BCFA) [21], which may be associated with disease [22] or beneficial impacts on host physiology [23]. Lipolysis of undigested dietary fat can lead to production of postbiotics with health-promoting effects to improve gut barrier integrity and reduce inflammatory conditions [24, 25], and commensal microbes generate bioactive lipids *de novo* that impact host physiology [26].

In this study, the physiological effect of consumption of identically formulated food processed under extrusion conditions generating either lower or higher concentrations of RS on microbiome saccharolysis, proteolysis, and lipolysis was examined in cats.

Materials and methods

Food production

Identically formulated foods (Table 1) that met the maintenance nutrition requirements outlined by the Association of American Feed Control Officials (AAFCO) and National Research Council were extruded with either high or low shear force. Extrusion was performed with a

Table 1. Study food formulation, proximate analysis, and digestibility.

| | LRS | HRS |
|---|--------------------|------|
| Ingredient, % dry matter | Formulation | |
| Poultry by-product meal (low ash) | 37.3 | |
| Brewer's rice | 18.5 | |
| Corn gluten meal | 11.8 | |
| Whole grain corn | 10.3 | |
| Pork fat | 9.9 | |
| Cellulose | 2.8 | |
| Palatant (spray-dried chicken) | 2.0 | |
| Lactic acid | 1.2 | |
| Palatant (liver digest) | 1.2 | |
| Potassium chloride | 1.1 | |
| Choline chloride | 0.9 | |
| Calcium sulfate | 0.8 | |
| Beet pulp | 0.7 | |
| Methionine, dL | 0.5 | |
| Vitamin E oil | 0.3 | |
| Palatant (dried yeast) | 0.2 | |
| Sodium chloride, iodized | 0.2 | |
| Vitamin mix | 0.2 | |
| Mineral mix | 0.1 | |
| Taurine | 0.1 | |
| Phosphoric acid | < 0.1 | |
| Proximate analysis, % | | |
| Moisture | 4.9 | 5.4 |
| Fat | 18.9 | 19.0 |
| Protein | 37.6 | 38.0 |
| Neutral detergent fiber | 9.7 | 8.4 |
| Ash | 6.1 | 6.1 |
| Crude fiber | 3.2 | 3.1 |
| Non-gelatinized starch (putative RS) | 0.5 | 7.9 |
| Digestibility | | |
| Apparent dry matter digestibility, % | 85.2 | 82.5 |
| Apparent protein digestibility, % | 86.8 | 83.0 |
| Apparent fat digestibility, % | 94.0 | 93.2 |
| Apparent fiber digestibility, % | 22.6 | 20.1 |
| Apparent NFE digestibility, % | 91.0 | 89.0 |
| Diet metabolic energy-AAFCO tested, kcal/kg | 4371 | 4286 |

AAFCO, Association of American Feed Control Officials; HRS, high resistant starch; LRS, low resistant starch; NFE, nitrogen-free extract.

<https://doi.org/10.1371/journal.pone.0241037.t001>

Wenger X-115 extruder (Wenger model 7 preconditioner; 115 mm outside diameter screw element) at the highest or lowest maximal shear rates that would provide a finished kibble with appropriate aesthetic properties. The higher specific mechanical energy in the high shear extrusion was due to high shaft rpm, low mass throughput, and reduced die open area (that increased the shear rate; [S1 Fig](#)). After extrusion, the formulations were dried and coated with palatants and fat.

Food and digestibility analyses

Before the trial described here, each food was initially screened for digestibility in separate digestibility feeding studies following the AAFCO quantitative collection protocol [27]. In these preliminary studies, animals were fed to maintain body weight, and water was freely available at all times. Each test included 6 adult cats and consisted of two phases: a pre-collection acclimation period of 9 days followed by a second phase lasting 5 days with total collection of feces. Analytical measurements for food-related energy, moisture, protein, fat, fiber, and ash and the corresponding nutrients in feces (fecal undigested nutrients) were performed as outlined by AAFCO. Crude fiber was measured according to the AOAC method 962.09. Digestibility coefficients for dry matter, nitrogen-free extract (NFE; putative digestible carbohydrate), and fiber were calculated as apparent digestibility [(consumed—fecal)/consumed]. Analytical measurements for food-related energy, moisture, protein, fat, fiber, and ash and the corresponding nutrients in feces were performed as outlined by AAFCO. Total dietary starch was approximated as putative digestible carbohydrate and is calculated from digestibility data as NFE, where $NFE = 100\% - (\text{crude fiber \%} + \text{crude protein \%} + \text{crude fat \%} + \text{ash \%} + \text{moisture \%})$. Percent cook quantitatively determines the degree of gelatinized starch in cereal-based foodstuffs based on the principle that gelatinized starch is readily digested by glucoamylase. Total starch is determined similarly with the exception that intact or raw starch in the sample is gelatinized prior to enzymatic digestion. Percent cook was determined on a YSI 2700 SELECT Biochemistry Analyzer (YSI Inc., Yellow Springs, Ohio, USA), and was calculated as $(\% \text{ gelatinized starch in food} / \% \text{ total starch in food}) \times 100$. Proximate analysis was carried out as previously described [28]. For rapid visco analysis (RVA), samples were frozen at -70°C , ground, and passed through a US#40 sieve [29]. Measured moisture was used to calculate sample size and water addition. Samples were run on a 23-minute profile and analyzed as previously described [30].

Animals and experimental design

Cats were individually housed in environments promoting social interaction, had access to natural light that varied with season, had daily opportunity to exercise and interact with caretakers, and were fed to maintain healthy body weight. The study protocol was reviewed and approved by the Institutional Animal Care and Use Committee, Hill's Pet Nutrition, Topeka, KS, USA (Protocol Number: FP644a.1.2.0-A-F-D-ADH-MULTI-91-GI), and complied with the National Institutes of Health guide for the care and use of laboratory animals as well as those from the US National Research Council and US Public Health Service [31]. All cats were domestic shorthair breed and were spayed or neutered. Cats were owned by the funders of this research, who gave permission for them to be included in this study. At the conclusion of the study, all cats were healthy and returned to the colony. Inclusion criteria was for healthy cats, considered as no evidence of chronic systemic disease in physical examination, complete blood count, serum biochemical analyses, urinalysis, or fecal examination for parasites. All cats completed the trial with no adverse events. Fresh food was offered daily with amounts calculated to maintain body weight, with electronic feeders that recorded daily food intake (g/day) for each cat; water was available ad libitum.

Cats were randomized by age, weight, and sex into two groups, where they received the high shear (low RS [LRS]) food or the low shear (high RS [HRS]) food (S1 Table). Caretakers were blinded to the food received, and each cat received only one of the foods. Body weight was assessed at baseline and every week for the duration of the study.

The study was a randomized, 7-week, longitudinal feeding trial with fecal collections carried out under IACUC-approved protocols. As felines do not reliably produce stools on a daily basis, two replicate fecal collections for each cat were attempted within a four-day period initiated at the outset of weeks 4 and 7. Analysis of IgA was carried out only on the first successful collection at week 7, and metabolomics analysis was only carried out on the first successful collection at both weeks 4 and 7. As initiation of stool collection occurred on the first day of weeks 4 and 7, there were 3 and 6 full weeks of feeding the experimental foods prior to sample collection periods. Hereafter, we refer to these collection timepoints as weeks 3 and 6. All cats were healthy following the study.

Fecal analysis

Stool production from cats is not regular or predictable. Therefore, in order to collect fresh feces, between the hours of 07:00 to 15:00 on collection days, caretakers visited the litter boxes every 15 minutes to assess production of stool. When a stool was observed, it was immediately scored on a 5-point scale on which a higher score indicates firmer stool [32]. After scoring, feces were extensively homogenized using a Planetary Centrifugal "Thinky Mixer" ARM-310 (Thinky U.S.A., Inc., Laguna Hills, CA, USA), and portions were flash frozen in liquid nitrogen within 30 minutes of defecation for SCFA, IgA, ammonia, metabolomic, and microbiome analysis. Fecal homogenate that was not flash frozen was analyzed for moisture, ash, and minerals. Organic dry matter was calculated as $100\% - (\text{moisture } \% + \text{ash } \%)$. Analysis of fecal moisture, ash, minerals, SCFA, metabolomics, and the composition of the fecal microbiome were carried out as previously described [28]. Fecal IgA was assessed using the feline IgA enzyme-linked immunosorbent assay quantitation set (Product #ab190547, AbCam; Cambridge, MA, USA) in which frozen fecal samples were lyophilized then mixed with extraction buffer prior to clarifying by centrifugation. Assay procedures were performed on collected supernatants according to the manufacturer's recommendations. Fecal ammonia was assayed from frozen wet feces. Briefly, fecal material was extracted with 2 M KCl, centrifuged, and the supernatant was subjected to reaction with Berthelot's reagent [33].

Microbiome data processing

Microbiome raw sequence data were processed as previously described [28]. Briefly, FASTQ files were obtained from a MiSeq instrument (Illumina, San Diego, CA, USA) in pairs. The files were pre-processed into contigs, chimeras removed, and bacterial taxonomic classification was obtained using Mothur software [34] using a modified protocol of the MiSeq SOP [35] published on the Mothur website [36] according to Greengenes reference taxonomy [37]. Operational taxonomic units (OTUs) were identified based on taxonomic hierarchy. Sequences were deposited in the NCBI Sequence Read Archive under accession number PRJNA63518.

Alpha diversity indices were calculated on genus-level count data in the R programming environment [38] using the R vegan package [39]. Alpha diversity indices are presented as Hill numbers [40] of order "q", corresponding to taxa richness (S; $q = 0$), exponential of the Shannon index ($\text{expH } q = 1$), and the inverse of the Simpson index ($\text{invSimp}; q = 2$). Respectively, these indices provide insight into microbiome community structure when taxa abundance is not considered (S), taxa contribute to the index according to their abundance (expH), and

highly abundant taxa contribute to a greater degree to the diversity value (invSimp). Pielou's Evenness (J) provides insight into the relative homogeneity of taxa abundance independent of the number of taxa detected [41]. In order to more fully assess the contribution of taxa abundance, Renyi alpha diversity series are reported, where increasing q denotes increasing influence of higher abundance taxa on diversity [42]. Beta diversity was calculated as $1 - CqN$ ($q\beta$) [43] and plotted on a continuum of increasing order q , in the same manner as for alpha diversity [44]. Renyi diversity series and $q\beta$ were generated with a custom R script [38] and are presented as curves for values of $0 < q < 10$, calculated at intervals of $q = 0.05$. This script uses the R shiny package [45] and is available upon request from the corresponding author.

Statistical analysis

For targeted endpoints, metabolomics and microbiome data the following statistical analyses were performed in JMP (versions 13.1–14.2. SAS Institute Inc., Cary, NC, 1989–2019): multivariate analysis of variance (MANOVA), independent t-test, and linear mixed modeling were employed to generate p values while partial least squares discriminant analysis (PLS-DA) was used to generate variable importance in projection (VIP) values using Nonlinear Iterative Partial Least Squares with 15 possible factors as the search space and K Fold cross validation ($K = 7$). Obtained metabolite and IgA values were \log_2 -transformed and statistics were performed on transformed values. Categorical ordinal stool scores were approximated as a continuous variable. Genus-level OTU count data were centered natural log-ratio (CLR) transformed [46] to enable multivariate operations on compositional data [47] using the `alder.clr` function in the R package ALDEx2 [48]. This operation consists of dividing the counts observed for an individual taxon by the geometric mean of counts for all observed taxa, followed by natural log transformation. Prior to CLR transformation, zero counts were inflated using Bayesian-multiplicative treatment [49] using the `CZM` attribute of the `cmultRepl` function in the R package `zCompositions` [50, 51]. For microbiome data, mixed modeling was carried out for weeks 3 and 6 separately with subject as random factor and using both week 3 and 6 timepoint data to test for an effect of RS across the entire study period with subject and collection number as random factors.

The sequential statistical process tested whether RS significantly impacted a given class of metabolites at either weeks 3 or 6, whether RS altered individual metabolites constituting as class at weeks 3 or 6, and finally whether there was an effect of RS on individual metabolites across the entire study. Determination of whether there was a difference by RS for a multivariate class of metabolites was performed separately at weeks 3 and 6 by MANOVA using the Identity function, which fits a model for each metabolite individually and then jointly tests the models together. Then, individual metabolites within a class were assessed at weeks 3 and 6 to determine which metabolites drove the significance observed for the class as a whole using t-tests when only one sample was analyzed per cat at each timepoint or linear mixed modeling when both collections at a timepoint were available. VIP scores were generated from PLS-DA and reported alongside p values at both weeks 3 and 6. To test for an effect of RS across the entire study period, linear mixed modeling was used with all data from both week 3 and 6 timepoints.

To account for the high dimensionality of the metabolite and genera-level microbiome data, false discovery-correcting q values were generated for all metabolites and genus level OTU in the R computing environment [38] using the "qvalue" function in the R package `qvalue` v2.14.1 [52] with separate vectors of p values from t-tests by timepoint and linear mixed modeling as input. Statistical significance was assigned to a metabolite or genera-level OTU where both of the following criteria were met: $p \leq 0.05$ and false discovery rate $q \leq 0.1$.

Global metabolome (log₂-transformed) and microbiome (CLR-transformed) analyses were carried out on the Metaboanalyst platform v4.0 [53]. Orthogonal partial least squares discriminant analysis (OPLS-DA; which included all 736 observed metabolites or 252 identified genus-level OTUs) with 2000 permutations as well as sparse partial least squares (SPLS; which included 20 metabolites or OTUs after dimensionality reduction), two components and 5-fold cross validation were carried out to detect metabolome- and microbiome-wide differences between HRS versus LRS-fed cats separately at weeks 3 and 6. Random forest was performed separately at each timepoint and in order to detect metabolite and genus-level OTU predictors of group identity (random forest number of trees = 2000, number of predictors = 10, randomness = on).

Results

Food production and analysis

Identically formulated foods (Table 1) were produced with either high or low shear extrusion force (S1 Fig). Percent cook analysis indicated that greater concentrations of RS were present in the low shear food (percent cook: high shear = 98.4%; low shear = 72.2%). Analysis of viscosity indicated a peak viscosity (indicative of cooked starch) of 1389 cP for high shear and 1009 cP for low shear, while final viscosity (which increases with higher molecular weight starch) was 1241 cP for high shear and 1780 cP for low shear. Together, these results indicate that the low shear extrusion conditions led to a food that contained less cooked starch with likely more RS and that its starch content was of a higher molecular weight. Hereafter, the foods produced by high and low shear are designated as low and high RS (LRS and HRS), respectively.

There were no nutritionally meaningful differences between the LRS and HRS foods in moisture, fat, protein, crude fiber, ash, or gross energy; neutral detergent fiber was marginally decreased in the HRS food (Table 1).

Study animals, food intake, and weight

Forty domestic short-haired breed cats were included in the study and split evenly between the LRS and HRS food groups, with a mean (SE) age of 8.9 (0.5) years (S1 Table). No stools were successfully collected from four cats during the monitoring periods at either weeks 3 or 6, and these cats were necessarily excluded from analysis.

Food digestibility and intake

There was no difference between the LRS and HRS foods for intake of calories ($P = 0.191$) or grams of food ($P = 0.347$) (S2 Table). There was also no difference between groups for intake of total starch, protein, or fat, nor was body weight changed from baseline for either group.

Results from pre-trial AAFCO quantitative collection protocol digestibility studies for each food showed no significant differences in digestibility by extrusion type, though the mean of each digestibility parameter was numerically lower for the HRS food (Table 1). Stool scores are measured as part of the digest study on a 5-point scale; moisture is also measured. In these preliminary digest studies, stool scores were not different when feeding HRS and LRS foods (stool score mean \pm SD: LRS, 4.25 \pm 0.53; HRS, 4.57 \pm 0.81; $P = 0.437$ by independent t-test). As well, stool moisture levels were not different between HRS- and LRS-fed cats in the preliminary digest studies (moisture mean \pm SD: LRS, 60.9 \pm 5.0; HRS, 64.8 \pm 5.8; $P = 0.244$ by independent t-test). Thus, both subjective, blinded stool scoring and objective fecal moisture data from the

preliminary digest trials indicated that RS feeding at the levels employed herein did not meaningfully affect stool firmness.

Stool scores and proximate analyses

Similar to the results of the preliminary digest studies, in the main feeding trial there was no difference in stool scores between the cats consuming LRS versus HRS foods at either week 3 (mean [SE], 4.81 [0.09] versus 4.69 [0.11], respectively; $P = 0.53$) or week 6 (4.94 [0.04] versus 4.84 [0.08], respectively; $P = 0.89$). There were, however, small but statistically significant increases in moisture (3.1–4.5% increased in HRS-fed cat feces, $P = 0.007$) offset by decreased organic dry matter in the feces of cats fed the HRS food (2.3–3.0% decreased, $P = 0.005$) (S3 Table). Taken together, stool scores and fecal moisture analyses showed little change with increased RS feeding in HRS-fed cats. The only fecal mineral consistently altered at both timepoints was potassium, which was increased in feces from HRS-fed cats, perhaps indicating a compensatory colonic osmoregulatory response to increased RS.

Fecal global metabolomics

Metabolomic analysis performed on fecal samples taken at weeks 3 and 6 identified 736 metabolites. Of these, 47% were significantly different ($P \leq 0.05$, $q \leq 0.1$) between the low and HRS foods by mixed modeling across both timepoints (36% increased and 11% decreased in the HRS food) (S3 Table). At week 3, 43% of metabolites had a PLS-DA VIP score > 1.0 (minimum root mean predictive residual sum of squares = 0.9, minimizing number of factors = 11, cumulative $Q^2 = 0.94$, cumulative $R^2Y = 0.99$) while at week 6, 41% of metabolites had a PLS-DA VIP score > 1.0 (minimum root mean predictive residual sum of squares = 0.41, minimizing number of factors = 3, cumulative $Q^2 = 0.98$, cumulative $R^2Y = 0.97$). The significant metabolite differences between the LRS and HRS-fed groups at week 3 were highly persistent to week 6 of feeding (week 3 \log_2FC versus week 6 \log_2FC Pearson correlation; adjusted $R^2 = 0.91$, $P < 0.001$, slope = 0.99).

OPLS analysis indicated greater metabolome-wide differences between cats fed LRS and HRS foods at week 6 than week 3; T-Scores and orthogonal T-Scores explained approximately 33% of variation at both weeks (Fig 1A and 1B). Dimensionality reduction of the number of discriminatory analytes from 736 to 20 using SPLS analysis on two components provided complete separation (S2 Fig; SPLS loadings are in S4 Table). Random forest analysis provided discrimination between the LRS and HRS food-fed cats at weeks 6 and 3 (overall out of bounds class error 5.7% and 17.1%, respectively; S3 Fig).

Based on the known actions of gut microbiota on undigested macronutrients, as well as prominence in the global metabolomics analysis, metabolites of carbohydrates, proteins, and lipids were further analyzed. Results in total show that most metabolite features of these nutrient classes were significantly different by dietary RS concentration (Table 2).

Saccharolysis and fermentation

RS- and epithelial-derived saccharides. Maltotriose, maltose, and glucose, known to be derived from microbial saccharolysis of RS, were increased in HRS-fed cats, but glucose was not increased at week 6 (Table 3). No RS-derived sugars were ever higher in the LRS group. Other, non-RS derived sugars increased in the HRS group (Table 3) including sugars typically associated with epithelial surfaces (mannose, N-acetylglucosaminylasparagine, glucuronate). No oligo- or monosaccharides were observed to be higher in the LRS group at either timepoint.

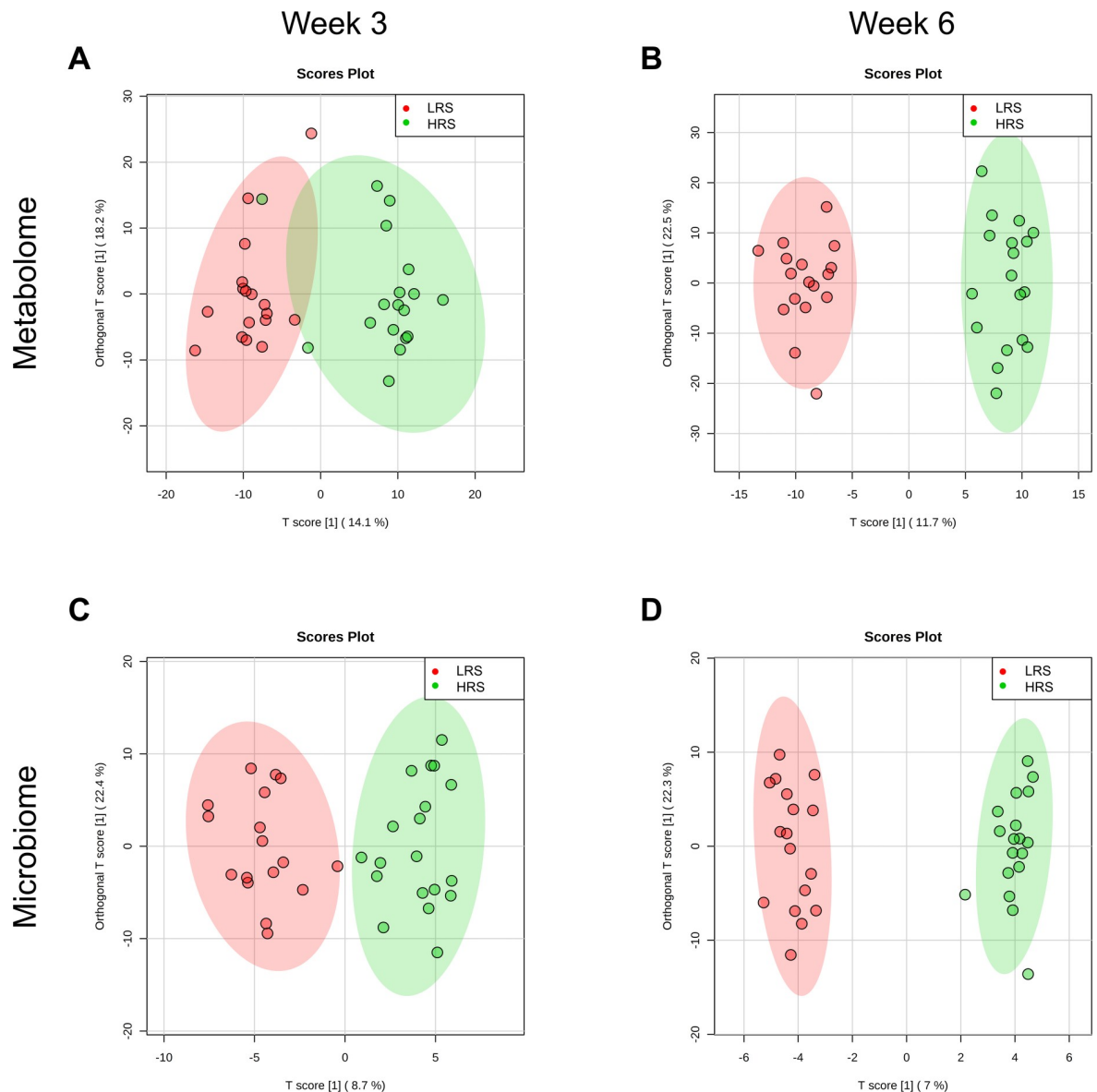


Fig 1. Orthogonal partial least squares analysis of whole fecal differences at weeks 3 and 6 between LRS and HRS food-fed cats for the metabolome (A,B) and microbiome (C,D). Shading indicates 95% confidence regions. Metabolome permutation statistics at week 3 were: $Q^2 = 0.38$, $P < 0.001$; $R^2Y = 0.80$, $P = 0.014$ and at week 6 were: $Q^2 = 0.86$, $P < 0.001$; $R^2Y = 0.96$, $P < 0.001$. Microbiome permutation statistics at week 3 were: $Q^2 P < 0.001$; $R^2Y P = 0.059$ and at week 6 were: $Q^2 P < 0.001$; $R^2Y P = 0.056$. HRS, high resistant starch; LRS, low resistant starch.

<https://doi.org/10.1371/journal.pone.0241037.g001>

SCFA production. At both weeks, the concentrations of the straight-chain SCFA butyrate and the ratio of total SCFA to total branched-chain SCFA were significantly higher in fecal samples from cats that consumed the HRS food (Table 4).

Five of the six straight- and branched-chain SCFAs quantified by targeted analysis were also observed as glycine conjugates in the metabolomics dataset (S3 Table); unconjugated SCFAs are typically not directly observed in metabolomic screens due to their volatility. Glycine conjugates of SCFA all increased while the BCFA conjugates isobutyrylglycine and isovalerylglycine decreased or were unchanged, respectively.

Table 2. Summary of metabolite class changes.

| Metabolism Type | Class | HRS/LRS |
|------------------|---------------------------|-------------------------------|
| Saccharolysis | RS sugars | ↑ |
| | other sugars | ↑ |
| Fermentation | SCFA | ↑ |
| | lactate | ↑ |
| Proteolysis | dipeptides | ↑ |
| | amino acids | ↑ |
| Putrefaction | ammonia | ↓ |
| | beneficial indoles | ↑ |
| | detrimental indoles | no change |
| | biogenic tryptophan amine | ↓ |
| | kynurenine | no change |
| | serotonin | ↓ |
| | polyamines | ↑ |
| Lipolysis | 1-acylglycerols | ↓ |
| | lysophospholipids | ↑ |
| | fatty acids | ↑ (saturated) ↓ (unsaturated) |
| | ketone body metabolism | ↑ |
| Bioactive lipids | N-acylethanolamines | ↓ |
| | 2-acylglycerols | ↓ |
| | NAD(H) precursors | ↑ |

HRS, high resistant starch; LRS, low resistant starch; NAD(H), nicotinamide adenine dinucleotide, oxidized or reduced form; SCFA, short-chain fatty acid.

<https://doi.org/10.1371/journal.pone.0241037.t002>

Proteolysis and putrefaction

Dipeptides and amino acids. Fecal concentrations of dipeptides, incomplete products of proteolysis, were significantly different as a class according to dietary RS concentration. There were 9/24 observed dipeptides significantly increased in the feces of HRS-fed cats across the entire study (Table 5). Amino acids were higher in the HRS group, an effect that increased from week 3 to 6 (Table 5). No dipeptides or amino acids were higher in the LRS group relative to the HRS group at either timepoint.

Ammonia. Fecal ammonia was significantly decreased at week 6 in the HRS group (\log_2 FC = -0.30, $P = 0.01$) but not at week 3 (S3 Table). Leucine metabolites isocaproate and isovalerate did not differ across groups, indicating that ammonia-generating Stickland fermentation was minimally affected by dietary RS concentration [54] (S3 Table). Similarly, increases in glycine betaine and sarcosine (S3 Table), both electron acceptors in Stickland reactions, were in opposition of those predicted if ammonia accumulation was substantial through this route [55].

Indoles. Indoles, putrefactive metabolites of tryptophan, were significantly different by RS at both weeks 3 and 6 (Table 6 and S3 Table). Notable were increases in indolelactate and indolepropionate. In contrast, indolin-2-one was decreased, and indoles hydroxylated on the aromatic ring as well as their sulfate conjugates were unchanged. Additional routes of metabolic disposal of tryptophan by gut microbes include the biogenic amine tryptamine, the kynurenine pathway, and serotonin production. Tryptamine and serotonin were both decreased in the feces from the HRS group, while kynurenines did not differ between groups (S3 Table).

Polyamines. Polyamines are products of microbial putrefaction of amino acids lysine, arginine, agmatine, and ornithine, with methylthioadenosine produced as a byproduct.

Table 3. Sugars derived from resistant starch and other sugars detected via metabolomic screening in fecal samples taken at weeks 3 and 6 from cats fed LRS or HRS food.

| Type | Metabolite | Week 3 | Week 6 |
|------------------------------|--------------------------------|----------|----------|
| | | Log2(FC) | Log2(FC) |
| RS sugar | glucose | | |
| | maltose | | |
| | maltotriose | | |
| | maltotetraose | | |
| Cell surface and plant sugar | mannose | | |
| | N-acetylglucosaminylasparagine | | |
| | glucuronate | | |
| | diacetylchitobiose | | |
| | fucose | | |
| | arabinose | | |
| | erythrose | | |
| | fructose | | |
| | ribose | | |
| | ribulose/xylulose | | |
| | sedoheptulose | | |
| | xylose | | |
| | erythronate | | |
| | threonate | | |

FC, fold-change of HRS/LRS; HRS, high resistant starch; LRS, low resistant starch.

Concentrations of a given metabolite in the HRS group versus the LRS group by independent t-test (week 3 or week 6) or mixed model (weeks 3 & 6) at $P < 0.05$ and $q < 0.1$ are shown as significantly higher (red), significantly lower (green), or unchanged (white). Full numerical data are available in [S3 Table](#).

<https://doi.org/10.1371/journal.pone.0241037.t003>

Polyamines and their catabolic intermediates were increased in the feces from HRS-fed cats at week 3 but not at week 6 (Table 6). The primary polyamines cadaverine (lysine-derived) and putrescine (arginine-, ornithine-, or agmatine-derived) were significantly increased in the

Table 4. Short-chain fatty acids in fecal samples taken at weeks 3 and 6 from cats fed LRS or HRS food.

| Fatty acid | Week 3 | | | | Week 6 | | | |
|------------------|----------------|----------------|---------|--------------------|----------------|----------------|---------|--------------------|
| | LRS | HRS | HRS-LRS | Independent t-test | LRS | HRS | HRS-LRS | Independent t-test |
| | Mean (SE) | Mean (SE) | Delta | p | Mean (SE) | Mean (SE) | Delta | p |
| Acetate | 2781.2 (266.7) | 3456.8 (269.6) | 675.6 | 0.087 | 2378.8 (240.1) | 2681.9 (193.1) | 303.1 | 0.338 |
| Propionate | 1289.8 (107.8) | 1460.8 (114.8) | 171.0 | 0.288 | 1033.1 (112.6) | 1165.1 (92.4) | 132.0 | 0.377 |
| Butyrate* | 1369.0 (120.9) | 2397.8 (183.7) | 1028.7 | < 0.001 | 1303.8 (93.2) | 1842.8 (171.6) | 539.0 | 0.013 |
| Isobutyrate | 282.0 (25.6) | 268.6 (20.2) | -13.4 | 0.685 | 281.6 (20.1) | 250.9 (17.7) | -30.7 | 0.265 |
| 2-methylbutyrate | 176.8 (17.4) | 169.4 (12.0) | -7.4 | 0.730 | 185.8 (17.5) | 165.8 (13.6) | -19.9 | 0.380 |
| Isovalerate | 342.7 (29.3) | 339.1 (22.8) | -3.6 | 0.923 | 350.4 (24.2) | 310.0 (20.2) | -40.4 | 0.216 |
| Total SCFA | 5440.0 (444.4) | 7315.4 (422.3) | 1875.4 | 0.005 | 4715.7 (396.8) | 5689.7 (359.2) | 974.1 | 0.084 |
| Total BCFA | 801.4 (71.9) | 777.0 (54.2) | -24.4 | 0.789 | 817.7 (61.4) | 726.8 (50.9) | -91.0 | 0.268 |
| SCFA/BCFA | 7.0 (0.5) | 9.9 (0.8) | 2.9 | 0.004 | 5.9 (0.5) | 8.2 (0.7) | 2.3 | 0.014 |

*Two subjects were removed from analysis as statistical outliers: values of 4229.4 (Subject 14) and 3107.2 ppm (Subject 35).

BCFA, branched -chain fatty acid; FC, fold change; HRS, high resistant starch; LRS, low resistant starch; SCFA, short-chain fatty acid; SE, standard error.

Assays were performed as previously described [28].

<https://doi.org/10.1371/journal.pone.0241037.t004>

Table 5. Dipeptides and amino acids detected via metabolomic screening in fecal samples taken at weeks 3 and 6 from cats fed LRS or HRS food.

| Type | Metabolite | Week 3 | Week 6 |
|-------------------|-----------------------|----------|----------|
| | | Log2(FC) | Log2(FC) |
| Dipeptide | alanylleucine | | |
| | cysteinylglycine | | |
| | glutaminylleucine | | |
| | glycylisoleucine | | |
| | glycylleucine | | |
| | glycylvaline | | |
| | histidylalanine | | |
| | isoleucylglycine | | |
| | leucylalanine | | |
| | leucylglutamine | | |
| | leucylglycine | | |
| | lysylleucine | | |
| | phenylalanylalanine | | |
| | phenylalanylglycine | | |
| | prolylglycine | | |
| | prolylhydroxyproline | | |
| | threonylphenylalanine | | |
| | tryptophylglycine | | |
| | tyrosylglycine | | |
| | valerylphenylalanine | | |
| valeryltryptophan | | | |
| valylglutamine | | | |
| valylglycine | | | |
| valylleucine | | | |
| Amino acid | alanine | | |
| | arginine | | |
| | asparagine | | |
| | aspartate | | |
| | cysteine | | |
| | glutamate | | |
| | glutamine | | |
| | glycine | | |
| | histidine | | |
| | isoleucine | | |
| | leucine | | |
| | lysine | | |
| | methionine | | |
| | phenylalanine | | |
| | proline | | |
| | serine | | |
| | taurine | | |
| | threonine | | |
| | tryptophan | | |
| | tyrosine | | |
| valine | | | |

FC, fold change; HRS, high resistant starch; LRS, low resistant starch.

Concentrations of a given metabolite in the HRS group versus the LRS group by independent t-test (week 3 or week 6) or mixed model (weeks 3 & 6) at $P < 0.05$ and $q < 0.1$ are shown as significantly higher (red), significantly lower (green), or unchanged (white). Full numerical data are available in [S3 Table](#).

<https://doi.org/10.1371/journal.pone.0241037.t005>

Table 6. Indoles and polyamines detected via metabolomic screening in fecal samples taken at weeks 3 and 6 from cats fed LRS or HRS food.

| Type | Metabolite | Week 3 | Week 6 |
|-----------|--------------------------------|----------|----------|
| | | Log2(FC) | Log2(FC) |
| Indole | 2-oxindole-3-acetate | | |
| | 3-hydroxyindolin-2-one | | |
| | 3-hydroxyindolin-2-one sulfate | | |
| | 3-indoxyl sulfate | | |
| | 5-hydroxyindoleacetate | | |
| | indole | | |
| | indoleacetate | | |
| | indoleacetyl glycine | | |
| | indolelactate | | |
| | indolepropionate | | |
| | indolin-2-one | | |
| | methyl indole-3-acetate | | |
| Polyamine | cadaverine | | |
| | N-acetyl-cadaverine | | |
| | putrescine | | |
| | N-acetylputrescine | | |
| | N-acetyl-isoptreanine | | |
| | spermidine | | |
| | diacetylspermidine | | |
| | (N(1) + N(8))-acetylspermidine | | |
| | N(1)-acetylspermine | | |
| | N1,N12-diacetylspermine | | |
| | carboxyethyl-GABA | | |

FC, fold change; GABA, gamma aminobutyric acid; HRS, high resistant starch; LRS, low resistant starch.

Concentrations of a given metabolite in the HRS group versus the LRS group by independent t-test (week 3 or week 6) or mixed model (weeks 3 & 6) at $P < 0.05$ and $q < 0.1$ are shown as significantly higher (red), significantly lower (green), or unchanged (white). Full numerical data are available in S3 Table.

<https://doi.org/10.1371/journal.pone.0241037.t006>

HRS group but spermidine was unchanged; spermine was not observed in the dataset. Although there were extensive increases in free amino acids in the HRS group (*vide supra*), neither arginine nor lysine precursors to polyamines were increased. Agmatine was not different by RS, but ornithine was increased in the HRS group (S3 Table). Methylthioadenosine, a byproduct of putrescine chain elongation, was increased in the HRS group (S3 Table).

Lipolysis and production of bioactive lipids

Lipolysis. Incomplete products of lipolysis were found to vary by RS at both timepoints; 1-monoacylglycerols increased while lysophospholipids decreased. Lysophospholipids derived from all three phospholipids (phosphatidylethanolamine, phosphatidylcholine, and phosphatidylserine) and containing both saturated (palmitoyl, stearoyl) as well as unsaturated (oleoyl, linoleoyl) acyl chains were increased in the feces from HRS-fed cats (S3 Table). Complete products of lipolysis, non-esterified fatty acids, varied by RS concentration depending on their chain length (S3 Table); the specific effects of RS feeding on long-chain polyunsaturated fatty acids were quite prominent. Of the six omega-3 (n3) NEFA observed in the dataset, four were persistently decreased in the HRS group at both weeks. Conversely, medium-chain saturated fats valerate, caproate, and heptanoate were increased by HRS feeding; since these are not

present at significant amounts in the diet, they are likely derived from β -oxidation of longer chain dietary fatty acids.

Ketogenesis. At both weeks 3 and 6, β -hydroxybutyrate (BHB) was increased in feces from HRS-fed cats (Table 7). Caproate (hexanoate), converted to BHB via the intermediacy of butyrate through β -oxidation by gut microbiota, was increased in feces from HRS-fed cats at both timepoints and the product of its β -oxidation, 3-hydroxyhexanoate, was also increased by mixed modeling across the study. As indicated above, the SCFA butyrate can undergo β -oxidation to form BHB, and this SCFA was increased in the HRS group. Together, these data indicate that a ketogenic state is potentially induced in the colonic lumen with RS feeding in cats.

Endocannabinoids. N-acylethanolamine endocannabinoids are products of mammalian and perhaps microbial metabolism. These cannabinoids were significantly decreased by RS feeding (Table 7), with an effect greater for the very long chain species. While 2-monoacylglycerols were decreased by RS feeding at 3 weeks, these transient effects contrasted with the persistent effect on very long-chain N-acylethanolamines.

Bile acids. As a multivariate class, bile acids significantly differed by RS at weeks 3 and 6 (S3 Table). Of the 23 primary and secondary bile acids detected in the fecal metabolomics data, 12 were increased in the feces from HRS-fed cats and only three decreased relative to the LRS group by mixed modeling across timepoints (Table 7). The effect for individual bile acids was similar across weeks 3 and 6; however, there was a trend toward decreased impact of RS on bile acids at the week 6 timepoint. The largest magnitudes of changes were increases in the primary bile acids cholate and taurocholate sulfate and the secondary bile acids 12-dehydrocholate, 3-dehydrocholate and a decrease in the secondary bile acid 6-oxolithocholate. The secondary bile acid deoxycholate was also significantly decreased across the study duration.

NADH-coupled hydroxyl:Oxo redox ratios

The ratio of NADH:NAD⁺-coupled hydroxyl:oxo redox pairs derived from gut microbial metabolism of both dietary carbohydrate and protein catabolism were increased in the HRS group, with a larger effect at week 6 than 3 (Table 8). The increased hydroxyl:oxo ratio stemmed from elevated concentrations of the reduced (hydroxyl) member of the redox couple; the oxidized (oxo) member of the redox couple did not differ across groups. This held true for redox couples derived from the microbiome-mediated metabolism of sugars and the amino acids isoleucine, leucine, valine, phenylalanine, as well as for hydroxyl metabolites of tryptophan metabolism indolelactate, imidazole lactate, and 3-(4-hydroxyphenyl)lactate (S3 Table). Since the relative concentrations of the hydroxyl:oxo forms of these redox ratio pairs are in equilibrium with the NADH:NAD⁺ redox couple, we examined the concentrations of all observed fecal metabolites containing a nicotinic moiety (S3 Table). Changes of the class related to NADH metabolism [56] were among the largest seen in this study and were also highly persistent across timepoints.

Fecal microbiome

A total of 406 OTUs were classified at the genus level in the fecal samples, including many with unknown genus identification. Of these, 252 OTUs were identified at the genus level and subjected to univariate statistical analysis by OTU; 30% were different for at least one time point and 21% were different across the study (S3 Table). Fold changes (FC) for LRS vs HRS present at week 3 were highly persistent to week 6 (week 3 $\ln[FC]$ versus week 6 $\ln[FC]$ Pearson correlation; adjusted $R^2 = 0.92$, $P < 0.001$, slope = 1.11). Mixed modeling assessment using data from both timepoints showed that changes in fecal OTUs that were significant at only one of the timepoints were supported by trends at the other timepoint.

Table 7. Ketogenic metabolites, ethanolamides, and bile acids detected via metabolomic screening in fecal samples taken at weeks 3 and 6 from cats fed LRS or HRS food.

| Type | Metabolite | Week 3 | Week 6 |
|-------------------------------|-----------------------------------|----------|----------|
| | | Log2(FC) | Log2(FC) |
| Ketogenesis | 3-hydroxybutyrate (BHB) | | |
| | 3-hydroxy-3-methylglutarate (HMG) | | |
| | caproate (6:0) | | |
| | 3-hydroxyhexanoate | | |
| Cannabinoid ethanolamide | palmitoyl ethanolamide | | |
| | palmitoleoyl ethanolamide | | |
| | margaroyl ethanolamide | | |
| | stearoyl ethanolamide | | |
| | oleoyl ethanolamide | | |
| | linoleoyl ethanolamide | | |
| | dihomo-linolenoyl ethanolamide | | |
| | arachidoyl ethanolamide (20:0) | | |
| | arachidonoyl ethanolamide | | |
| | behenoyl ethanolamide (22:0) | | |
| | erucoyl ethanolamide (22:1) | | |
| | lignoceroyl ethanolamide (24:0) | | |
| nervonoyl ethanolamide (24:1) | | | |
| Bile acid | chenodeoxycholate | | |
| | cholate | | |
| | cholate sulfate | | |
| | glycochenodeoxycholate | | |
| | hyocholate | | |
| | taurochenodeoxycholate | | |
| | taurocholate | | |
| | taurochenate sulfate | | |
| | ursocholate | | |
| | 12-dehydrocholate | | |
| | 3-dehydrocholate | | |
| | 6-oxolithocholate | | |
| | 7-ketodeoxycholate | | |
| | 7-ketolithocholate | | |
| | dehydrolithocholate | | |
| | deoxycholate | | |
| | glycodeoxycholate | | |
| | glycolithocholate | | |
| | isohyodeoxycholate | | |
| | isoursodeoxycholate | | |
| lithocholate | | | |
| taurodeoxycholate | | | |
| tauroolithocholate 3-sulfate | | | |

FC, fold change; HRS, high resistant starch; LRS, low resistant starch.

Concentrations of a given metabolite in the HRS group versus the LRS group by independent t-test (week 3 or week 6) or mixed model (weeks 3 & 6) at $P < 0.05$ and $q < 0.1$ are shown as significantly higher (red), significantly lower (green), or unchanged (white). Full numerical data are available in [S3 Table](#).

<https://doi.org/10.1371/journal.pone.0241037.t007>

Table 8. Redox-coupled congeners detected via metabolomic screening in fecal samples taken at weeks 3 and 6 from cats fed LRS or HRS food.

| Source | Redox Ratios and Congeners | Week 3 | Week 6 |
|---------------|--|----------|----------|
| | | Log2(FC) | Log2(FC) |
| Sugar | lactate/pyruvate* | | |
| | lactate | | |
| | pyruvate | | |
| Isoleucine | 2-hydroxy-3-methylvalerate/3-methyl-2-oxovalerate* | | |
| | 2-hydroxy-3-methylvalerate | | |
| | 3-methyl-2-oxovalerate | | |
| Leucine | alpha-hydroxyisocaproate/4-methyl-2-oxopentanoate* | | |
| | alpha-hydroxyisocaproate | | |
| | 4-methyl-2-oxopentanoate | | |
| Valine | alpha-hydroxyisovalerate/3-methyl-2-oxobutyrate* | | |
| | alpha-hydroxyisovalerate | | |
| | 3-methyl-2-oxobutyrate | | |
| Phenylalanine | phenyllactate/phenylpyruvate* | | |
| | phenyllactate (PLA) | | |
| | phenylpyruvate | | |

*Derived ratios were not included in q value estimation.

FC, fold change; HRS, high resistant starch; LRS, low resistant starch.

Concentrations of a given metabolite in the HRS versus the LRS group by independent t-test (week 3 or week 6) or mixed model (weeks 3 & 6) at $P < 0.05$ and $q < 0.1$ are shown as significantly higher (red), significantly lower (green), or unchanged (white). Full numerical data are available in [S3 Table](#).

<https://doi.org/10.1371/journal.pone.0241037.t008>

Subsequent to Aitchison transformation with the CLR function [47], a global microbiome assessment was carried out. OPLS assessment of the CLR-transformed 252 genus-level classified OTUs showed complete separation of the 95% confidence regions of the HRS versus LRS groups at both weeks 3 and 6. The T-Score and orthogonal T-Score explained approximately 30% of variation at both timepoints (Fig 1C and 1D). Dimensionality reduction of the number of analytes using SPLS analysis provided separation of the 95% confidence regions at both weeks 3 and 6 and accounted for approximately 24% and 15% of variation, respectively (S2 Fig). There were nine OTUs in common in component 1 of both timepoints, indicating that these genera were persistently discriminatory for RS consumption in cats. Among these nine OTUs were saccharolytic (*Lactobacillus*) and proteolytic (*Peptococcus*, *Peptostreptococcus*) bacteria as well as methanogenic Archaea (*Methanosarcina*) (S4 Table). Random forest analysis provided a marginally better classification of the groups at week 6 than week 3 (overall out of bounds class error, 14.3% and 19.4%, respectively; S4 Fig). Members of phylum Firmicutes were prominent predictors of dietary RS concentration; at both weeks 3 and 6, eight of the top 20 ranked OTU were genera in this phylum, while members of phylum Bacteroidetes only accounted for 3/20 top ranked features. There were 11 genera in common and six of these were from phylum Firmicutes while only two were from phylum Bacteroidetes in the union of the 3 and 6 week random forest classifier data. The genera from phylum Firmicutes had both saccharolytic (*Lactobacillus*, *Blautia*, *Megasphaera*) and proteolytic (*Peptococcus*, *Peptostreptococcus*) proclivities. When assessed at the phylum level, the Bacteroidetes:Firmicutes ratio was significantly lower in the microbiomes of the HRS group across the study and at each timepoint (S3 Table). Analysis at the phylum level also showed that the most strongly increased phylum in the HRS group was Acidobacteria, which appears to be consistent with the observation of increased fecal lactic acid (lactate) in this group.

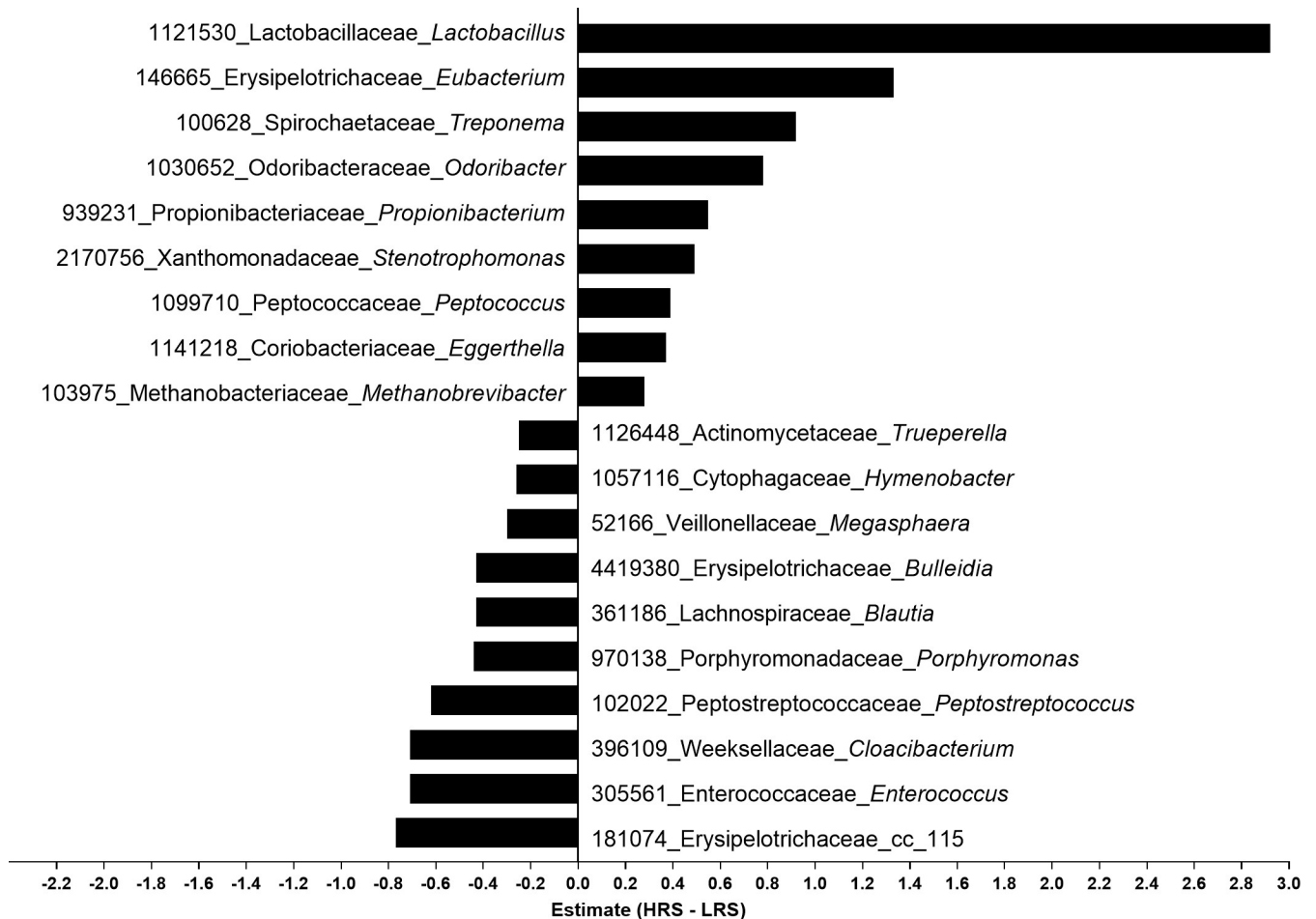


Fig 2. Significant genus-level taxa differences in the fecal microbiome from consumption of HRS or LRS food using a mixed model of weeks 3 and 6. Subject and collection number were random factors. Operational taxonomic unit number, family, and genus are shown for those with the greatest differences; full data are available in [S3 Table](#). HRS, high resistant starch; LRS, low resistant starch.

<https://doi.org/10.1371/journal.pone.0241037.g002>

The most prominent differences in individual taxa by mixed modeling were decreases in the genera *Enterococcus*, *Peptostreptococcus*, and *Megasphaera*, while *Porphyromonas*, *Acidaminococcus*, *Blautia*, *Ruminococcus*, and *Peptoniphilus* were decreased less consistently across the study. Prominently increased genera were *Lactobacillus*, *Eubacterium*, *Odoribacter*, *Treponema*, *Stenotrophomonas*, and *Peptococcus* (Fig 2; S3 Table). Thus, abundances of genera associated with both saccharolytic and proteolytic process were markedly altered by consumption of RS in the HRS food, consistent with the observed changes to both saccharolytic/fermentative and proteolytic/putrefactive metabolites.

Community structure was assessed, using all 406 OTUs classified at the genera level, by way of diversity indices based on the total number of observed taxa as well as relative abundances of those taxa. Analysis of alpha diversity showed that there was persistently higher diversity in the fecal microbiome of cats consuming the HRS versus LRS foods in a manner that persisted across the timepoints (Table 9). Taxa richness (S) was significantly higher in the HRS group at both weeks 3 and 6. The exponent of Shannon index (expH) and the inverse of Simpson index (invSimp) were also increased at weeks 3 and 6. Pielou's Evenness (J) was not different at either timepoint, although there was a trend towards increased evenness when assessed across both

Table 9. Alpha diversity metrics from fecal samples from cats fed LRS or HRS food.

| Alpha Diversity Index | Week 3 | | | | Week 6 | | | |
|-----------------------|---------------|---------------|---------|--------------|---------------|---------------|---------|--------------|
| | LRS | HRS | HRS-LRS | Mixed Model* | LRS | HRS | HRS-LRS | Mixed Model* |
| | Mean (SE) | Mean (SE) | Delta | p value | Mean (SE) | Mean (SE) | Delta | p value |
| S | 104.63 (2.44) | 109.42 (1.90) | 4.78 | 0.004 | 102.85 (3.21) | 110.66 (2.76) | 7.81 | 0.004 |
| expH | 16.92 (0.79) | 21.06 (0.84) | 4.15 | 0.027 | 16.98 (0.67) | 20.50 (0.66) | 3.52 | 0.034 |
| invSimp | 10.04 (0.51) | 12.34 (0.68) | 2.30 | 0.003 | 10.34 (0.50) | 12.21 (0.53) | 1.87 | 0.013 |
| J | 0.60 (0.01) | 0.64 (0.01) | 0.04 | 0.221 | 0.61 (0.01) | 0.64 (0.01) | 0.03 | 0.099 |

*Subject as a random factor. † Subject and collection number as random factors.

expH, exponential of the Shannon index; HRS, high resistant starch; invSimp, inverse of the Simpson index; J, Pielou's evenness; LRS, low resistant starch; S, taxa richness; SE, standard error.

Data are presented as mean (SE).

<https://doi.org/10.1371/journal.pone.0241037.t009>

timepoints ($P = 0.073$). The percent mean increase in diversity of the HRS group from the LRS group for both the Shannon and Simpson diversity indices was approximately the same (~24% at 3 weeks, ~20% at 6 weeks for both expH and invSimp). To better gain insight into the degree to which taxa abundance impacted observed differences in alpha diversity, a sweep of diversity values from $0 < q < 10$ at intervals of $q = 0.05$ was carried out using data from the week 3 and 6 timepoints. Mixed modeling indicated that the HRS group manifested higher alpha diversity until $q = 5$, beyond which there were not significant differences by shear type (S5 Table). Beta diversity (1-CqN; $q\beta$) was assessed along the same continuum of order q ($0 < q < 10$), and the $q\beta$ curve of HRS-fed cats was markedly higher than that of the LRS group in the range of $2.5 < q < 8$ (S5 Table).

Fecal secretory IgA

In order to assess the degree to which RS feeding impacted the host-microbiome mutualistic relationship, IgA was assessed in feces at week 6. Fecal IgA concentrations from cats fed the HRS food were significantly higher at week 6 compared with those fed the LRS food (S3 Table).

Discussion

This study examined the effects of feline consumption of RS produced through different extrusion conditions on gut microbiome metabolism of dietary carbohydrate, protein, and fat. The starch in the HRS food was 27% less cooked as assessed by independent methods (percent cook and viscosity analysis) and its molecular weight was 40% higher, the result of a 60% reduction of extrusion shear force. The effect of RS consumption on feline gut microbiome metabolism was pervasive and persistent; nearly 50% of the fecal metabolome was altered and these differences were highly correlated across time points. There was no overt effect on stool firmness as assessed by stool quality score and fecal moisture, and stool macro and mineral analyses were minimally impacted, indicating the feasibility of intervening with dietary RS in domestic cats to produce sizeable shifts in microbiome function without producing wide deviations in stool firmness or composition.

In the current study, RS consumption provided carbohydrates for gut microbial saccharolysis and fermentation. RS-derived substrates for saccharolysis were increased in feces alongside the saccharolytic products of epithelial cell polysaccharides [57, 58]. There was a greater effect as time progressed perhaps indicating adaptation to RS consumption. On a molar basis, RS is a particularly efficient precursor of butyrate production [59] and has been shown to ameliorate proteinuria in a mouse model of CKD [60], aspects that may be beneficial to diabetic cats,

which have a paucity of butyrate-producing bacteria in their microbiome [61]. Increased fecal butyrate in the HRS diet group indicates the potential for dietary RS to exert a benefit in cats. Dietary RS is also a known source of lactate production by lactic acid bacteria, with the lactate used for subsequent production of butyrate [62, 63]. Increased lactate in the current study in HRS-fed cats may have contributed to the increased concentration of butyrate that was observed. Bacteria complexed with IgA, which is secreted into the luminal space of the colon and binds to gut commensals, promote gut homeostasis and induce a more robust and pervasive effect on host physiology than uncomplexed bacteria [64, 65]. Dietary RS consumption increases IgA in rats [66, 67], mice [68], and pigs [69], an effect that may be driven by SCFA production [70].

Proteolytic and putrefactive metabolites of protein also appeared in feces. Undigested protein delivered to the colon is subject to microbial proteolysis, and postbiotics derived from putrefaction of amino acids are reabsorbed into systemic circulation [71]. Dietary RS increased concentrations of dipeptide and amino acid products of proteolysis. However, ammonia, which is a marker of microbial amino acid putrefaction [72], decreased in the HRS-fed cats. Products of ammonia-generating Stickland fermentation were not different by RS concentration, while concentrations of electron acceptors for these reactions indicated reduced activity through this pathway. This may indicate that the increased carbohydrate availability and fermentation with RS feeding lessened microbial putrefaction, as has been previously observed [73], and that putrefaction to generate ammonia [21] was decreased by RS feeding.

Products of amino acid putrefaction are associated with detrimental health consequences, particularly for renal-impaired individuals [74, 75], also demonstrated in cats [76]. However, protein escaping digestion does not necessarily have negative consequences to health [77] and can provide benefits [78–80]; undigested protein has previously been shown to increase gut microbial butyrate and IgA [81, 82], as well as heighten the effect of dietary RS to increase microbial production of SCFA [83]. Gut microbial metabolites of tryptophan [23, 84, 85] have beneficial health effects on gut and systemic physiology [77]. In the current study, higher RS increased fecal indole-3-propionate, a gut microbe metabolite of tryptophan that improves gut barrier integrity [86] and interferes with metabolism by pathogens [87]. Indole-3-lactate, produced by *Bifidobacterium* species [88], has anti-inflammatory activity [89], and is converted to indole-3-propionate, was also increased in the HRS-fed cats. Previous reports show RS feeding increased indole-3-lactate and indole-3-acetate in serum of CKD rats, although these were decreased or unchanged in cecal contents [90]. Tryptophan-derived biogenic amine tryptamine and serotonin were decreased by RS feeding while kynurenines were unchanged. Serotonin can influence gut motility and thus transit time of food and stool firmness. Commensal microbiota partially determine concentrations of colonic serotonin in an SCFA-dependent manner by direct synthesis [91], stimulation of release from enterochromaffin cells and by modulating reuptake by serotonin transporters [92]. Though the cats enrolled in this study were healthy, and stool firmness was not impacted by RS feeding, the finding that RS feeding reduces fecal serotonin concentrations in cats may hold promise for recommendation of diets for management of feline subjects with chronic watery stools.

Gut microbiota synthesize polyamines from arginine and its derivatives as well as lysine, cadaverine, putrescine, and spermidine [1, 93]. Microbial production of polyamines abrogates the detrimental impact of aging on intestinal epithelia [94, 95] and may serve protective roles against endothelial dysfunction [96] and neoplastic processes [97]. Cadaverine, putrescine, and acetylated forms of spermidine were increased by HRS food although whether cats may benefit from RS through increased polyamine production remains to be tested.

Although fat is typically highly digestible and absorbed in healthy subjects, products of partial and complete lipolysis were observed in feces alongside bioactive lipids. The ratio of dietary

fat to starch has been shown to influence the microbiome composition and function in dogs [98]. Dietary fat that escapes digestion is available in the colon as a nutrient source for resident bacteria [99], and gut commensals harbor capacity for degradation of fatty acids [100] via β -oxidation [101]. Gut microbial β -oxidation converts longer chain fatty acids to SCFA (e.g., butyrate) and medium chain fatty acids (MCFA; e.g., caproate). SCFA and MCFA are absorbed into colonocytes, but MCFA absorption *in vivo* is twice as great as that of SCFA and its catabolism equals or exceeds that of SCFA [102]. Ketogenesis, an aspect of fat metabolism, is related to the host-microbiome physiology; both SCFA and MCFA are ketogenic as they are converted to the ketone body BHB in colonocytes [102, 103]. In addition to their provision of butyrate and MCFA as precursors of colonocyte BHB, gut microbes also directly generate and metabolize ketone bodies [104, 105]. Feeding of diets enriched with RS has been previously shown to increase BHB in canine feces [106] as well as in mouse plasma [107] and rat serum [90]. In this study, RS feeding significantly increased fecal concentrations of BHB. Additional substrates for production of BHB via β -oxidation, including butyrate, caproate, and 3-hydroxyhexanoate, were increased as well. As BHB inhibits neutrophil inflammasome activation [108] and activates the G-protein coupled receptor GPR109 with multitudinous metabolic benefits [109], RS might benefit colon health of cats by supporting a ketogenic colonic milieu. Co-production of butyrate alongside BHB has been proposed to generate synergistic health benefits [110]; since RS feeding increased both butyrate and BHB in the current study, these synergistic benefits might generally extend to cats consuming RS.

In addition to fatty acid catabolism, commensal gut microbes also synthesize bioactive lipid species that mimic host signaling molecules. The gut microbiome harbors diverse N-acyl amide synthases [26], and microbiota generate N-acylethanolamides [111, 112] with potential to impact host physiology [113]. Activation of the endocannabinoid pathway by N-acylethanolamides leads to loss of gut barrier integrity and metabolic endotoxemia [114], and endocannabinoids interact with the gut microbiome [115]. Feeding of prebiotic fiber has previously been reported to increase gene expression of fatty acid amide hydrolase (FAAH, degrading endocannabinoid N-acylethanolamines), decreasing arachidonylethanolamide and restoring gut barrier integrity while decreasing circulating endotoxin [114]. In this study, we observed that RS feeding decreased a broad swath of very long chain endocannabinoid N-acylethanolamines (≥ 20 carbons). Since phosphatidylethanolamines were increased, RS feeding might have reduced their conversion to N-acylethanolamines. Alternatively, prebiotic RS might have increased catabolism of N-acylethanolamines by FAAH [114]. Taken together, RS feeding in the HRS group had a consistent effect to decrease very long-chain N-acylethanolamine endocannabinoids.

As in humans, cats generate primary bile acids while colonic microbiota convert these to secondary bile acids [116] with implications for host physiology. Bile acids bind the nuclear farnesoid X receptor and modulate the innate immune system to induce tolerance of the host to resident gut microbes [117, 118]. Although dysregulated production of bile acids can promote colon carcinogenic processes [119], secondary bile acids have been reported to accumulate in tumor tissue to decrease tumor growth and increase patient survival [120]. In this study, the increase of primary bile acids in the HRS-fed cats was persistent, while the effect of RS on secondary bile acids decreased over time. One of the decreases observed across the study was for the secondary bile acid deoxycholate, which activates the enzyme responsible for hydrolyzing N-acylphosphatidylethanolamines to endocannabinoid N-acylethanolamines [121]. As deoxycholate was decreased in the HRS group, consequent reduction of hydrolase activity might provide a mechanism whereby endocannabinoid N-acylethanolamines decreased while phosphatidylethanolamine phospholipids increased.

The unifying biochemical directive that may be shaping the microbial metabolism of undigested carbohydrate and protein in this study appears to be the redox balance of saccharolytic

and proteolytic metabolites in equilibrium with NADH:NAD⁺ (or NADPH:NADP⁺). The hydroxyl:oxo ratio of a diverse set of microbial metabolites was significantly increased in the HRS group. Consistent with these metabolites being in equilibrium with NADH:NAD⁺, we also observed that metabolites containing the nicotinic moiety and serving as precursors to NADH synthesis were strongly increased in the HRS group. These same metabolites are used therapeutically to increase NAD(H) concentrations in vivo [56]. To our knowledge, this unified shift in NADH:NAD⁺ coupled fecal redox state has not been previously reported. It may be that the availability of ample reducing equivalents produced through microbiome catabolism of RS drives this shift of toward increased hydroxyl:oxo ratios. Monocarboxylate transporters can carry ionized redox couples into colonocytes from the luminal environment [122]. Lactate:pyruvate and associated hydroxyl:oxo redox couples may serve as two-electron shuttles, enabling communication of the redox state of the microbial milieu to the host and equilibration of NADH:NAD⁺ between commensals and colonocytes. Additionally, high concentrations of lactate and NADH shift the equilibrium away from ADP-ribosylation and its concomitant detrimental effects, including toxin activity of pathogenic bacteria [123] and inflammation [124], while promoting tissue repair [125]. Although untested in this study, based on known NAD⁺ biology, microbiota from the HRS-fed cats generating high ratios of lactate:pyruvate (accompanied by high ratios of NADH:NAD⁺) may exhibit decreased post-translational ADP-ribosylation of proteins since NAD⁺ is the source of ADP-ribose for this process [123].

There was a persistent impact of RS feeding on the fecal microbiome of cats, but RS feeding impacted a smaller percentage of bacterial genera than it did fecal metabolites. Additionally, where the bulk of changes to the metabolome were increases in the HRS-fed cats, the majority of changes to genus-level OTU were decreases. Increased fecal lactate is consistent with the microbiome data, in that a prominent lactate producer (*Lactobacillus*) was the most highly increased genus and a lactate consumer (*Megasphaera*) were among the top ten decreased genera in the HRS group at both weeks 3 and 6. Members of the phylum Acidobacteria were increased, consistent with the predilection of these bacteria for environments with lower pH as might be expected when lactate concentrations increase. Regarding proteolysis, two genera in family Peptostreptococcaceae were decreased in the HRS-fed cats (*Peptostreptococcus* and *Tepidibacter*), while *Peptococcus* in family Peptococcaceae was increased. The ratio of Bacteroidetes:Firmicutes was decreased by RS feeding in this study, while genera in the Firmicutes phylum consistently served as classifiers of RS intake. In a previous study, an increased Bacteroidetes:Firmicutes ratio in rats with CKD was seen after RS feeding [90], although the RS form used in that study was pelleted rather than extruded and thus was of a more uniform structure and homogenous molecular weight than that generated by extrusion in the current study. Those authors proposed that feeding of a uniform and homogenous RS form may have led to their observation that RS decreased microbiome diversity. In contrast, our diversity data show that several metrics of microbiome community alpha diversity, including taxa richness as well as both Shannon and Simpson indices, were increased with HRS-food feeding. Assessment of alpha diversity on a continuum indicate that increases may have been driven largely by taxa with low- to mid-range abundances rather than by differences between groups of the most abundant taxa. Taxa of intermediate abundance were the greatest contributors to differences in beta diversity.

A strength of this study is the longitudinal design whereby the persistence of the effects of dietary RS in cats can be assessed. As well, results of the preliminary digest studies, stool scoring and fecal moisture data, and food intakes show that it is feasible to implement processing modifications impacting microbiome and metabolomic features without detrimentally deteriorating stool quality, digestibility, or food acceptance. Since reduced starch cook can be

associated with decreased stool firmness, it may be that in the current trial the CF and NDF levels stemming from added cellulose and beet pulp abrogated deteriorations in stool firmness that might otherwise have occurred with the relatively low percent cook of the HRS food.

A caveat to the study is that absolute concentrations of RS in the foods may have been overestimated as RS was measured in the food as ungelatinized and high molecular weight starch through enzymatic percent cook and viscosity analyses, although this should not affect the relative comparisons between intakes between groups (e.g., ratio of RS intake between HRS and LRS groups). It may, however, detrimentally impact the ability to compare to other publications that report RS per se rather than RVA or percent cook. Also, a confounding source of prebiotics in the diet was non-RS fiber. We only measured fiber in the diet as crude fiber and neutral detergent fiber, both of which may underrepresent total dietary fiber. While crude fiber was not different between the foods, neutral detergent fiber was approximately 13% decreased in the HRS food, which may have contributed in part to observed differences.

In summary, this study is the first to examine the effects of RS intake on the fecal metabolome and microbiome of cats. Cats necessarily require higher protein intakes than canine companion animals, and this predisposes them to microbial production of putrefactives with detrimental consequences to health. Provision of a grain-rich feline adult maintenance formula with a higher RS:protein ratio that reaches the colon can shift microbial metabolism toward generation of postbiotics known to benefit gut and renal health and decrease production of metabolites detrimental to health. The consumption of RS increased fecal butyrate, ketones, indolelactate/indolepropionate, polyamines, and host production of IgA while also decreasing ammonia and endocannabinoids. As ammonia was decreased when amino acid appearance in feces was heightened, and hydroxyindoles associated with renal insufficiency were unchanged between groups, it does not appear that putrefaction to detrimental postbiotics occurred to any meaningful extent. Also, the balance of saccharolytic to proteolytic bacteria was shifted in a way that provides a mechanism to underpin the observed differences in metabolites. Cats, which are obligate carnivores, can benefit from consumption of a grain-based food that contains substantial RS.

Supporting information

S1 Fig. Extrusion under (A) LRS and (B) HRS conditions.
(TIF)

S2 Fig. Sparse partial least squares analysis of whole fecal differences at weeks 3 and 6 between LRS and HRS food-fed cats for the metabolome (A,B) and microbiome (C,D). Shading indicates 95% confidence regions.
(TIF)

S3 Fig. Random forest analysis of predictors of metabolomic group differences at (A) week 3 and (B) week 6.
(TIF)

S4 Fig. Random forest analysis of predictors of group differences in the microbiome at (A) week 3 and (B) week 6. Operational taxonomic unit number, family, genus, and species (where known) are shown.
(TIF)

S1 Table. Baseline characteristics, group assignments, and stool collections for cats in the study.
(DOCX)

S2 Table. Mean food intakes and undigested nutrients.
(DOCX)

S3 Table. Mean values at weeks 3 and 6 in fecal proximate analysis, minerals, short-chain fatty acids, selected metabolomics, IgA, and microbiome in cats fed LRS or HRS food.
(XLSX)

S4 Table. Loadings for sparse partial least squares analysis for the metabolome and microbiome at weeks 3 and 6.
(XLSX)

S5 Table. Alpha and beta diversity plots versus order q.
(XLSX)

Acknowledgments

The authors gratefully acknowledge the caretakers at Hill's Pet Nutrition Science and Technology Center, Topeka, KS, 66617 for care and welfare of the cats and for timely collections. Jennifer L. Giel, PhD, assisted with the development of the manuscript.

Author Contributions

Conceptualization: Matthew I. Jackson, Christopher Waldy, Dennis E. Jewell.

Formal analysis: Matthew I. Jackson.

Investigation: Matthew I. Jackson, Christopher Waldy, Dennis E. Jewell.

Methodology: Matthew I. Jackson, Christopher Waldy, Dennis E. Jewell.

Project administration: Matthew I. Jackson.

Writing – original draft: Matthew I. Jackson.

Writing – review & editing: Christopher Waldy, Dennis E. Jewell.

References

1. Matsumoto M, Ooga T, Kibe R, Aiba Y, Koga Y, Benno Y. Colonic absorption of low-molecular-weight metabolites influenced by the intestinal microbiome: A pilot study. *PLoS One*. 2017; 12: e0169207. <https://doi.org/10.1371/journal.pone.0169207> PMID: 28121990
2. Martinez KB, Leone V, Chang EB. Microbial metabolites in health and disease: Navigating the unknown in search of function. *J Biol Chem*. 2017; 292: 8553–9. <https://doi.org/10.1074/jbc.R116.752899> PMID: 28389566
3. Heintz-Buschart A, Wilmes P. Human gut microbiome: function matters. *Trends Microbiol*. 2018; 26: 563–74. <https://doi.org/10.1016/j.tim.2017.11.002> PMID: 29173869
4. Omosibi MO, Osundahunsi OF, Fagbemi TN. Effect of extrusion on protein quality, antinutritional factors, and digestibility of complementary diet from quality protein maize and soybean protein concentrate. *J Food Biochem*. 2018; 42: e12508.
5. Clarke E, Wiseman J. Effects of extrusion conditions on trypsin inhibitor activity of full fat soybeans and subsequent effects on their nutritional value for young broilers. *Br Poult Sci*. 2007; 48: 703–12. <https://doi.org/10.1080/00071660701684255> PMID: 18085453
6. Ralet M-C, Thibault J-F, Della Valle G. Solubilization of sugar-beet pulp cell wall polysaccharides by extrusion-cooking. *Lebensmittel-Wissenschaft und-Technologie*. 1991; 24: 107–12.
7. Tran QD, Hendriks WH, van der Poel AFB. Effects of extrusion processing on nutrients in dry pet food. *J Sci Food Agri*. 2008; 88: 1487–93.
8. Sajilata MG, Singhal RS, Kulkarni PR. Resistant starch- a review. *Compr Rev Food Sci Food Saf*. 2006; 5: 1–17.

9. Guha M, Ali Z. Molecular degradation of starch during extrusion cooking of rice. *Int J Food Prop*. 2002; 5: 50–521.
10. Maier TV, Lucio M, Lee LH, VerBerkmoes NC, Brislawn CJ, Bernhardt J, et al. Impact of dietary resistant starch on the human gut microbiome, metaproteome, and metabolome. *mBio*. 2017; 8.
11. Peixoto MC, Ribeiro EM, Maria APJ, Loureiro BA, di Santo LG, Putarov TC, et al. Effect of resistant starch on the intestinal health of old dogs: fermentation products and histological features of the intestinal mucosa. *J Anim Physiol Anim Nutr (Berl)*. 2018; 102: e111–e21. <https://doi.org/10.1111/jpn.12711> PMID: 28444804
12. Brahma S, Weier SA, Rose DJ. Moisture content during extrusion of oats impacts the initial fermentation metabolites and probiotic bacteria during extended fermentation by human fecal microbiota. *Food Res Int*. 2017; 97: 209–14. <https://doi.org/10.1016/j.foodres.2017.04.019> PMID: 28578043
13. Barry KA, Middelbos IS, Vester Boler BM, Dowd SE, Suchodolski JS, Henrissat B, et al. Effects of dietary fiber on the feline gastrointestinal metagenome. *J Proteome Res*. 2012; 11: 5924–33. <https://doi.org/10.1021/pr3006809> PMID: 23075436
14. Eshar D, Lee C, Weese JS. Comparative molecular analysis of fecal microbiota of bobcats (*Lynx rufus*) and domestic cats (*Felis catus*). *Can J Vet Res*. 2019; 83: 42–9. PMID: 30670901
15. Butowski CF, Thomas DG, Young W, Cave NJ, McKenzie CM, Rosendale DI, et al. Addition of plant dietary fibre to a raw red meat high protein, high fat diet, alters the faecal bacteriome and organic acid profiles of the domestic cat (*Felis catus*). *PLoS One*. 2019; 14: e0216072. <https://doi.org/10.1371/journal.pone.0216072> PMID: 31042730
16. Rochus K, Janssens GP, Hesta M. Dietary fibre and the importance of the gut microbiota in feline nutrition: a review. *Nutr Res Rev*. 2014; 27: 295–307. <https://doi.org/10.1017/S0954422414000213> PMID: 25623083
17. Pinna C, Stefanelli C, Biagi G. In vitro effect of dietary protein level and nondigestible oligosaccharides on feline fecal microbiota. *J Anim Sci*. 2014; 92: 5593–602. <https://doi.org/10.2527/jas.2013-7459> PMID: 25367521
18. Barry KA, Wojcicki BJ, Middelbos IS, Vester BM, Swanson KS, Fahey GC Jr. Dietary cellulose, fructooligosaccharides, and pectin modify fecal protein catabolites and microbial populations in adult cats. *J Anim Sci*. 2010; 88: 2978–87. <https://doi.org/10.2527/jas.2009-2464> PMID: 20495116
19. Herrmann E, Young W, Reichert-Grimm V, Weis S, Riedel CU, Rosendale D, et al. In vivo assessment of resistant starch degradation by the caecal microbiota of mice using rna-based stable isotope probing—a proof-of-principle study. *Nutrients*. 2018; 10. <https://doi.org/10.3390/nu10020179> PMID: 29415499
20. Aguilar-Toaláa JE, Garcia-Varelab R, Garcia HS, Mata-Harod V, González-Córdovaa AF, Vallejo-Cordobaa B, et al. Postbiotics: An evolving term within the functional foods field. *Trends Food Sci Technol*. 2018; 75: 105–14.
21. Smith EA, Macfarlane GT. Dissimilatory amino acid metabolism in human colonic bacteria. *Anaerobe*. 1997; 3: 327–37. <https://doi.org/10.1006/anae.1997.0121> PMID: 16887608
22. Rettger LF. Studies on putrefaction. *J Biol Chem*. 1906; 2: 71–86.
23. Galligan JJ. Beneficial actions of microbiota-derived tryptophan metabolites. *Neurogastroenterol Motil*. 2018; 30. <https://doi.org/10.1111/nmo.13283> PMID: 29341448
24. Miyamoto J, Mizukure T, Park SB, Kishino S, Kimura I, Hirano K, et al. A gut microbial metabolite of linoleic acid, 10-hydroxy-cis-12-octadecenoic acid, ameliorates intestinal epithelial barrier impairment partially via GPR40-MEK-ERK pathway. *J Biol Chem*. 2015; 290: 2902–18. <https://doi.org/10.1074/jbc.M114.610733> PMID: 25505251
25. Kaikiri H, Miyamoto J, Kawakami T, Park SB, Kitamura N, Kishino S, et al. Supplemental feeding of a gut microbial metabolite of linoleic acid, 10-hydroxy-cis-12-octadecenoic acid, alleviates spontaneous atopic dermatitis and modulates intestinal microbiota in NC/nga mice. *Int J Food Sci Nutr*. 2017; 68: 941–51. <https://doi.org/10.1080/09637486.2017.1318116> PMID: 28438083
26. Cohen LJ, Esterhazy D, Kim SH, Lemetre C, Aguilar RR, Gordon EA, et al. Commensal bacteria make GPCR ligands that mimic human signalling molecules. *Nature*. 2017; 549: 48–53. <https://doi.org/10.1038/nature23874> PMID: 28854168
27. Association of American Feed Control Officials. 2019 Official Publication Champaign, IL. Available from: <https://www.aafco.org/Publications>.
28. Jackson MI, Jewell DE. Balance of saccharolysis and proteolysis underpins improvements in stool quality induced by adding a fiber bundle containing bound polyphenols to either hydrolyzed meat or grain-rich foods. *Gut Microbes*. 2019; 10: 298–320. <https://doi.org/10.1080/19490976.2018.1526580> PMID: 30376392
29. The RVA Handbook. St. Paul, MN: AACC International; 2007.

30. Martinez MM. Applications of the rapid visco analyser (RVA) in the food industry: a broader view [Internet]. 2015 [cited 23 January 2019]. Available from: <https://www.perten.com/Publications/Articles/Applications-of-the-Rapid-Visco-Analyser-RVA-in-the-Food-Industry-a-broader-view/>.
31. National Research Council Committee Update of the Guide for the Care and Use of Laboratory Animals. The National Academies Collection: Reports funded by National Institutes of Health. Washington (DC): National Academies Press (US), National Academy of Sciences; 2011.
32. Hall JA, Melendez LD, Jewell DE. Using gross energy improves metabolizable energy predictive equations for pet foods whereas undigested protein and fiber content predict stool quality. *PLoS One*. 2013; 8: e54405. <https://doi.org/10.1371/journal.pone.0054405> PMID: 23342151
33. Chaney AL, Marbach EP. Modified reagents for determination of urea and ammonia. *Clin Chem*. 1962; 8: 130–2. PMID: 13878063
34. Schloss PD, Westcott SL, Ryabin T, Hall JR, Hartmann M, Hollister EB, et al. Introducing mothur: open-source, platform-independent, community-supported software for describing and comparing microbial communities. *Appl Environ Microbiol*. 2009; 75: 7537–41. <https://doi.org/10.1128/AEM.01541-09> PMID: 19801464
35. Kozich JJ, Westcott SL, Baxter NT, Highlander SK, Schloss PD. Development of a dual-index sequencing strategy and curation pipeline for analyzing amplicon sequence data on the MiSeq Illumina sequencing platform. *Appl Environ Microbiol*. 2013; 79: 5112–20. <https://doi.org/10.1128/AEM.01043-13> PMID: 23793624
36. MiSeq SOP [Internet]. 2017 [cited 2017 November 3]. Available from: https://www.mothur.org/wiki/MiSeq_SOP.
37. DeSantis TZ, Hugenholtz P, Larsen N, Rojas M, Brodie EL, Keller K, et al. Greengenes, a chimera-checked 16S rRNA gene database and workbench compatible with ARB. *Appl Environ Microbiol*. 2006; 72: 5069–72. <https://doi.org/10.1128/AEM.03006-05> PMID: 16820507
38. R Core Team. R: A language and environment for statistical computing [Internet]. Vienna, Austria: R Foundation for Statistical Computing; 2018 [cited 20 January 2019]. Available from: <http://www.R-project.org/>.
39. Oksanen J, Blanchet FG, Friendly M, Kindt R, Legendre P, McGlenn D, et al. vegan: Community Ecology Package. R package version 2.4–6. [Internet]. 2018 [cited 20 January 2019]. Available from: <https://CRAN.R-project.org/package=vegan>.
40. Hill MO. Diversity and evenness: a unifying notation and its consequences. *Ecology*. 1973; 54: 427–32.
41. Jost L. The relation between evenness and diversity. *Diversity*. 2010; 2: 207–32.
42. Tothmeresz B. Comparison of different methods for diversity ordering. *J Veg Sci*. 1995; 6: 283–90.
43. Jost L, Chao A, Chazdon RL. Compositional similarity and beta diversity. In: Magurran AE, McGill BJ, editors. *Biological diversity: frontiers in measurement and assessment*. New York: Oxford University Press; 2011. p. 66–84.
44. Gotelli NJ, Chao A. Measuring and estimating species richness, species diversity, and biotic similarity from sampling data. In: Levin SA, editor. *Encyclopedia of Biodiversity*. Second ed: Academic Press; 2013. p. 195–211.
45. Chang W, Cheng J, Allaire JJ, Xie Y, McPherson J, RStudio, et al. shiny: web application framework for R [Internet]. 2018 [cited 5 July 2019]. Available from: <https://CRAN.R-project.org/package=shiny>.
46. Aitchison J. Principles of compositional data analysis. In: Anderson TW FK, and Olkin I, editors, editor. *Multivariate analysis and its applications*. 24. Hayward (CA): Institute of Mathematical Statistics; 1994. p. 73–81.
47. Gloor GB, Macklaim JM, Pawlowsky-Glahn V, Egozcue JJ. Microbiome Datasets Are Compositional: And This Is Not Optional. *Front Microbiol*. 2017; 8: 2224. <https://doi.org/10.3389/fmicb.2017.02224> PMID: 29187837
48. Gloor G, Wong RG, Fernandes A, Albert A, Links M, Quinn T, et al. ALDEx2 Package. R package version 1.10.0. [Internet]. 2017 [cited 10 October 2018]. Available from: <https://bioconductor.org/packages/release/bioc/html/ALDEx2.html>.
49. Martin-Fernandez JA, Hron K, Templ M, Filzmoser P, Palarea-Albaladejo J. Bayesian-multiplicative treatment of count zeros in compositional data sets. *Statistical Modelling*. 2015; 15: 134–58.
50. Palarea-Albaladejo J, Martín-Fernández A. zCompositions—R package for multivariate imputation of left-censored data under a compositional approach. *Chemometr Intell Lab Syst*. 2015; 143: 85–96.
51. Palarea-Albaladejo J, Martín-Fernández A. zCompositions: treatment of zeros, left-censored and missing values in compositional data sets [Internet]. 2018 [cited 10 October 2018]. Available from: <https://CRAN.R-project.org/package=zCompositions>.

52. Storey JD, Bass AJ, Dabney A, Robinson D. qvalue: Q-value estimation for false discovery rate control [Internet]. 2014 [cited 12 May 2019]. Available from: <http://github.com/jdstorey/qvalue>.
53. Chong J, Soufan O, Li C, Caraus I, Li S, Bourque G, et al. MetaboAnalyst 4.0: towards more transparent and integrative metabolomics analysis. *Nucleic Acids Res.* 2018; 46: W486–w94. <https://doi.org/10.1093/nar/gky310> PMID: 29762782
54. Britz ML, Wilkinson RG. Leucine dissimilation to isovaleric and isocaproic acids by cell suspensions of amino acid fermenting anaerobes: the Stickland reaction revisited. *Can J Microbiol.* 1982; 28: 291–300. <https://doi.org/10.1139/m82-043> PMID: 6805929
55. Naumann E, Hippe H, Gottschalk G. Betaine: New oxidant in the Stickland reaction and methanogenesis from betaine and L-alanine by a *Clostridium sporogenes*-*Methanosarcina barkeri* coculture. *Appl Environ Microbiol.* 1983; 45: 474–83. <https://doi.org/10.1128/AEM.45.2.474-483.1983> PMID: 16346196
56. Katsyuba E, Auwerx J. Modulating NAD(+) metabolism, from bench to bedside. *EMBO J.* 2017; 36: 2670–83. <https://doi.org/10.15252/embj.201797135> PMID: 28784597
57. Hoskins LC, Boulding ET, Gerken TA, Harouny VR, Kriaris MS. Mucin glycoprotein degradation by mucin oligosaccharide-degrading strains of human faecal bacterial: characterization of saccharide cleavage products and their potential role in nutritional support of larger faecal bacterial populations. *Microb Ecol Health Dis.* 1992; 5: 193–207.
58. Pickard JM, Chervonsky AV. Intestinal fucose as a mediator of host-microbe symbiosis. *J Immunol.* 2015; 194: 5588–93. <https://doi.org/10.4049/jimmunol.1500395> PMID: 26048966
59. Pryde SE, Duncan SH, Hold GL, Stewart CS, Flint HJ. The microbiology of butyrate formation in the human colon. *FEMS Microbiol Lett.* 2002; 217: 133–9. <https://doi.org/10.1111/j.1574-6968.2002.tb11467.x> PMID: 12480096
60. Felizardo RJF, de Almeida DC, Pereira RL, Watanabe IKM, Doimo NTS, Ribeiro WR, et al. Gut microbial metabolite butyrate protects against proteinuric kidney disease through epigenetic- and GPR109a-mediated mechanisms. *FASEB J.* 2019: fj201901080R. <https://doi.org/10.1096/fj.201901080R> PMID: 31366236
61. Kieler IN, Osto M, Hugentobler L, Puetz L, Gilbert MTP, Hansen T, et al. Diabetic cats have decreased gut microbial diversity and a lack of butyrate producing bacteria. *Sci Rep.* 2019; 9: 4822. <https://doi.org/10.1038/s41598-019-41195-0> PMID: 30886210
62. Bourriaud C, Robins RJ, Martin L, Kozlowski F, Tenailleau E, Cherbut C, et al. Lactate is mainly fermented to butyrate by human intestinal microfloras but inter-individual variation is evident. *J Appl Microbiol.* 2005; 99: 201–12. <https://doi.org/10.1111/j.1365-2672.2005.02605.x> PMID: 15960680
63. Duncan SH, Louis P, Flint HJ. Lactate-utilizing bacteria, isolated from human feces, that produce butyrate as a major fermentation product. *Appl Environ Microbiol.* 2004; 70: 5810–7. <https://doi.org/10.1128/AEM.70.10.5810-5817.2004> PMID: 15466518
64. Mikulic J, Longet S, Favre L, Benyacoub J, Corthesy B. Secretory IgA in complex with *Lactobacillus rhamnosus* potentiates mucosal dendritic cell-mediated Treg cell differentiation via TLR regulatory proteins, RALDH2 and secretion of IL-10 and TGF-beta. *Cell Mol Immunol.* 2017; 14: 546–56. <https://doi.org/10.1038/cmi.2015.110> PMID: 26972771
65. Sun J, Qi C, Zhu H, Zhou Q, Xiao H, Le G, et al. IgA-targeted *Lactobacillus jensenii* modulated gut barrier and microbiota in high-fat diet-fed mice. *Front Microbiol.* 2019; 10: 1179. <https://doi.org/10.3389/fmicb.2019.01179> PMID: 31178854
66. Morita T, Tanabe H, Sugiyama K, Kasaoka S, Kiriya S. Dietary resistant starch alters the characteristics of colonic mucosa and exerts a protective effect on trinitrobenzene sulfonic acid-induced colitis in rats. *Biosci Biotechnol Biochem.* 2004; 68: 2155–64. <https://doi.org/10.1271/bbb.68.2155> PMID: 15502362
67. Morita T, Tanabe H, Takahashi K, Sugiyama K. Ingestion of resistant starch protects endotoxin influx from the intestinal tract and reduces D-galactosamine-induced liver injury in rats. *J Gastroenterol Hepatol.* 2004; 19: 303–13. <https://doi.org/10.1111/j.1440-1746.2003.03208.x> PMID: 14748878
68. Tanaka M, Honda Y, Miwa S, Akahori R, Matsumoto K. Comparison of the effects of roasted and boiled red kidney beans (*Phaseolus vulgaris* L.) on glucose/lipid metabolism and intestinal immunity in a high-fat diet-induced murine obesity model. *J Food Sci.* 2019; 84: 1180–7. <https://doi.org/10.1111/1750-3841.14583> PMID: 30990903
69. Trachsel J, Briggs C, Gabler NK, Allen HK, Loving CL. Dietary resistant potato starch alters intestinal microbial communities and their metabolites, and markers of immune regulation and barrier function in swine. *Front Immunol.* 2019; 10: 1381. <https://doi.org/10.3389/fimmu.2019.01381> PMID: 31275319
70. Kim M, Qie Y, Park J, Kim CH. Gut microbial metabolites fuel host antibody responses. *Cell Host Microbe.* 2016; 20: 202–14. <https://doi.org/10.1016/j.chom.2016.07.001> PMID: 27476413

71. Dodd D, Spitzer MH, Van Treuren W, Merrill BD, Hryckowian AJ, Higginbottom SK, et al. A gut bacterial pathway metabolizes aromatic amino acids into nine circulating metabolites. *Nature*. 2017; 551: 648–52.
72. Richardson AJ, McKain N, Wallace RJ. Ammonia production by human faecal bacteria, and the enumeration, isolation and characterization of bacteria capable of growth on peptides and amino acids. *BMC Microbiol*. 2013; 13: 6. <https://doi.org/10.1186/1471-2180-13-6> PMID: 23312016
73. He X, Sun W, Ge T, Mu C, Zhu W. An increase in corn resistant starch decreases protein fermentation and modulates gut microbiota during in vitro cultivation of pig large intestinal inocula. *Anim Nutr*. 2017; 3: 219–24. <https://doi.org/10.1016/j.aninu.2017.06.004> PMID: 29767145
74. Vanholder R, Schepers E, Pletinck A, Nagler EV, Glorieux G. The uremic toxicity of indoxyl sulfate and p-cresyl sulfate: a systematic review. *J Am Soc Nephrol*. 2014; 25: 1897–907. <https://doi.org/10.1681/ASN.2013101062> PMID: 24812165
75. Gao H, Liu S. Role of uremic toxin indoxyl sulfate in the progression of cardiovascular disease. *Life Sci*. 2017; 185: 23–9. <https://doi.org/10.1016/j.lfs.2017.07.027> PMID: 28754616
76. Summers SC, Quimby JM, Isaiah A, Suchodolski JS, Lunghofer PJ, Gustafson DL. The fecal microbiome and serum concentrations of indoxyl sulfate and p-cresol sulfate in cats with chronic kidney disease. *J Vet Intern Med*. 2019; 33: 662–9. <https://doi.org/10.1111/jvim.15389> PMID: 30561098
77. Diether NE, Willing BP. Microbial fermentation of dietary protein: an important factor in diet-microbe-host interaction. *Microorganisms*. 2019; 7.
78. Kato N, Iwami K. Resistant protein; its existence and function beneficial to health. *J Nutr Sci Vitaminol (Tokyo)*. 2002; 48: 1–5.
79. Matsumoto J, Erami K, Ogawa H, Doi M, Kishida T, Ebihara K. Hypocholesterolemic effects of microbial protease-resistant fraction of Katsuobushi in ovariectomized rats depend on the both oil and undigested protein. *J Nutr Sci Vitaminol (Tokyo)*. 2007; 53: 508–14. <https://doi.org/10.3177/jnsv.53.508> PMID: 18202539
80. Sugano M, Goto S, Yamada Y, Yoshida K, Hashimoto Y, Matsuo T, et al. Cholesterol-lowering activity of various undigested fractions of soybean protein in rats. *J Nutr*. 1990; 120: 977–85. <https://doi.org/10.1093/jn/120.9.977> PMID: 2398419
81. Morita T, Kasaoka S, Hase K, Kiriyaama S. Oligo-L-methionine and resistant protein promote cecal butyrate production in rats fed resistant starch and fructooligosaccharide. *J Nutr*. 1999; 129: 1333–9. <https://doi.org/10.1093/jn/129.7.1333> PMID: 10395595
82. Okazaki Y, Tomotake H, Tsujimoto K, Sasaki M, Kato N. Consumption of a resistant protein, sericin, elevates fecal immunoglobulin A, mucins, and cecal organic acids in rats fed a high-fat diet. *J Nutr*. 2011; 141: 1975–81. <https://doi.org/10.3945/jn.111.144246> PMID: 21940508
83. Morita T, Kasaoka S, Ohhashi A, Ikai M, Numasaki Y, Kiriyaama S. Resistant proteins alter cecal short-chain fatty acid profiles in rats fed high amylose cornstarch. *J Nutr*. 1998; 128: 1156–64. <https://doi.org/10.1093/jn/128.7.1156> PMID: 9649600
84. Roager HM, Licht TR. Microbial tryptophan catabolites in health and disease. *Nat Commun*. 2018; 9: 3294. <https://doi.org/10.1038/s41467-018-05470-4> PMID: 30120222
85. Agus A, Planchais J, Sokol H. Gut microbiota regulation of tryptophan metabolism in health and disease. *Cell Host Microbe*. 2018; 23: 716–24. <https://doi.org/10.1016/j.chom.2018.05.003> PMID: 29902437
86. Venkatesh M, Mukherjee S, Wang H, Li H, Sun K, Benechet AP, et al. Symbiotic bacterial metabolites regulate gastrointestinal barrier function via the xenobiotic sensor PXR and Toll-like receptor 4. *Immunity*. 2014; 41: 296–310. <https://doi.org/10.1016/j.immuni.2014.06.014> PMID: 25065623
87. Negatu DA, Yamada Y, Xi Y, Go ML, Zimmerman M, Ganapathy U, et al. Gut microbiota metabolite indole propionic acid targets tryptophan biosynthesis in *Mycobacterium tuberculosis*. *mBio*. 2019; 10. <https://doi.org/10.1128/mBio.02781-18> PMID: 30914514
88. Aragazzini F, Ferrari A, Pacini N, Gualandris R. Indole-3-lactic acid as a tryptophan metabolite produced by *Bifidobacterium* spp. *Appl Environ Microbiol*. 1979; 38: 544–6. <https://doi.org/10.1128/AEM.38.3.544-546.1979> PMID: 533277
89. Aoki-Yoshida A, Ichida K, Aoki R, Kawasumi T, Suzuki C, Takayama Y. Prevention of UVB-induced production of the inflammatory mediator in human keratinocytes by lactic acid derivatives generated from aromatic amino acids. *Biosci Biotechnol Biochem*. 2013; 77: 1766–8. <https://doi.org/10.1271/bbb.120979> PMID: 23924721
90. Kieffer DA, Piccolo BD, Vaziri ND, Liu S, Lau WL, Khazaali M, et al. Resistant starch alters gut microbiome and metabolomic profiles concurrent with amelioration of chronic kidney disease in rats. *Am J Physiol Renal Physiol*. 2016; 310: F857–71. <https://doi.org/10.1152/ajprenal.00513.2015> PMID: 26841824

91. O'Mahony SM, Clarke G, Borre YE, Dinan TG, Cryan JF. Serotonin, tryptophan metabolism and the brain-gut-microbiome axis. *Behav Brain Res*. 2015; 277: 32–48. <https://doi.org/10.1016/j.bbr.2014.07.027> PMID: 25078296
92. Spohn SN, Mawe GM. Non-conventional features of peripheral serotonin signalling—the gut and beyond. *Nat Rev Gastroenterol Hepatol*. 2017; 14: 412–20. <https://doi.org/10.1038/nrgastro.2017.51> PMID: 28487547
93. Nakamura A, Ooga T, Matsumoto M. Intestinal luminal putrescine is produced by collective biosynthetic pathways of the commensal microbiome. *Gut Microbes*. 2019; 10: 159–71. <https://doi.org/10.1080/19490976.2018.1494466> PMID: 30183487
94. Kibe R, Kurihara S, Sakai Y, Suzuki H, Ooga T, Sawaki E, et al. Upregulation of colonic luminal polyamines produced by intestinal microbiota delays senescence in mice. *Sci Rep*. 2014; 4: 4548. <https://doi.org/10.1038/srep04548> PMID: 24686447
95. Matsumoto M, Kurihara S, Kibe R, Ashida H, Benno Y. Longevity in mice is promoted by probiotic-induced suppression of colonic senescence dependent on upregulation of gut bacterial polyamine production. *PLoS One*. 2011; 6: e23652. <https://doi.org/10.1371/journal.pone.0023652> PMID: 21858192
96. Matsumoto M, Kitada Y, Naito Y. Endothelial function is improved by inducing microbial polyamine production in the gut: A randomized placebo-controlled trial. *Nutrients*. 2019; 11. <https://doi.org/10.3390/nu11051188> PMID: 31137855
97. Kovacs T, Miko E, Vida A, Sebo E, Toth J, Csonka T, et al. Cadaverine, a metabolite of the microbiome, reduces breast cancer aggressiveness through trace amino acid receptors. *Sci Rep*. 2019; 9: 1300.
98. Schauf S, de la Fuente G, Newbold CJ, Salas-Mani A, Torre C, Abecia L, et al. Effect of dietary fat to starch content on fecal microbiota composition and activity in dogs. *J Anim Sci*. 2018.
99. Agans R, Gordon A, Kramer DL, Perez-Burillo S, Rufian-Henares JA, Paliy O. Dietary fatty acids sustain the growth of the human gut microbiota. *Appl Environ Microbiol*. 2018; 84. <https://doi.org/10.1128/AEM.01525-18> PMID: 30242004
100. Jimenez-Diaz L, Caballero A, Segura A. Pathways for the degradation of fatty acids in bacteria. In: Rojo F, editor. *Aerobic Utilization of Hydrocarbons, Oils and Lipids*: Springer International Publishing; 2017.
101. Iram SH, Cronan JE. The beta-oxidation systems of *Escherichia coli* and *Salmonella enterica* are not functionally equivalent. *J Bacteriol*. 2006; 188: 599–608. <https://doi.org/10.1128/JB.188.2.599-608.2006> PMID: 16385050
102. Jorgensen JR, Fitch MD, Mortensen PB, Fleming SE. In vivo absorption of medium-chain fatty acids by the rat colon exceeds that of short-chain fatty acids. *Gastroenterology*. 2001; 120: 1152–61. <https://doi.org/10.1053/gast.2001.23259> PMID: 11266379
103. Fitch MD, Fleming SE. Metabolism of short-chain fatty acids by rat colonic mucosa in vivo. *Am J Physiol*. 1999; 277: G31–40. <https://doi.org/10.1152/ajpgi.1999.277.1.G31> PMID: 10409148
104. Pauli G, Overath P. *ato* operon: a highly inducible system for acetoacetate and butyrate degradation in *Escherichia coli*. *Eur J Biochem*. 1972; 29: 553–62. <https://doi.org/10.1111/j.1432-1033.1972.tb02021.x> PMID: 4563344
105. Aneja P, Dziak R, Cai GQ, Charles TC. Identification of an acetoacetyl coenzyme A synthetase-dependent pathway for utilization of L-(+)-3-hydroxybutyrate in *Sinorhizobium meliloti*. *J Bacteriol*. 2002; 184: 1571–7. <https://doi.org/10.1128/jb.184.6.1571-1577.2002> PMID: 11872708
106. Kim YJ, Kim JG, Lee WK, So KM, Kim JK. Trial data of the anti-obesity potential of a high resistant starch diet for canines using Dodamssal rice and the identification of discriminating markers in feces for metabolic profiling. *Metabolomics*. 2019; 15: 21. <https://doi.org/10.1007/s11306-019-1479-4> PMID: 30830428
107. Koay YC, Wali JA, Luk AWS, Macia L, Cogger VC, Pulpitel TJ, et al. Ingestion of resistant starch by mice markedly increases microbiome-derived metabolites. *FASEB J*. 2019; 33: 8033–42. <https://doi.org/10.1096/fj.201900177R> PMID: 30925066
108. Goldberg EL, Asher JL, Molony RD, Shaw AC, Zeiss CJ, Wang C, et al. beta-hydroxybutyrate deactivates neutrophil nlrp3 inflammasome to relieve gout flares. *Cell Rep*. 2017; 18: 2077–87. <https://doi.org/10.1016/j.celrep.2017.02.004> PMID: 28249154
109. Newman JC, Verdin E. beta-hydroxybutyrate: much more than a metabolite. *Diabetes Res Clin Pract*. 2014; 106: 173–81. <https://doi.org/10.1016/j.diabres.2014.08.009> PMID: 25193333
110. Cavaleri F, Bashar E. Potential synergies of beta-hydroxybutyrate and butyrate on the modulation of metabolism, inflammation, cognition, and general health. *J Nutr Metab*. 2018; 2018: 7195760. <https://doi.org/10.1155/2018/7195760> PMID: 29805804

111. Cohen LJ, Kang HS, Chu J, Huang YH, Gordon EA, Reddy BV, et al. Functional metagenomic discovery of bacterial effectors in the human microbiome and isolation of commendamide, a GPCR G2A/132 agonist. *Proc Natl Acad Sci U S A*. 2015; 112: E4825–34. <https://doi.org/10.1073/pnas.1508737112> PMID: 26283367
112. Lynch A, Crowley E, Casey E, Cano R, Shanahan R, McGlacken G, et al. The Bacteroidales produce an N-acylated derivative of glycine with both cholesterol-solubilising and hemolytic activity. *Sci Rep*. 2017; 7: 13270. <https://doi.org/10.1038/s41598-017-13774-6> PMID: 29038461
113. Burstein SH. N-acyl amino acids (elmiric acids): endogenous signaling molecules with therapeutic potential. *Mol Pharmacol*. 2018; 93: 228–38. <https://doi.org/10.1124/mol.117.110841> PMID: 29138268
114. Muccioli GG, Naslain D, Backhed F, Reigstad CS, Lambert DM, Delzenne NM, et al. The endocannabinoid system links gut microbiota to adipogenesis. *Mol Syst Biol*. 2010; 6: 392. <https://doi.org/10.1038/msb.2010.46> PMID: 20664638
115. Moludi J, Alizadeh M, Lotfi Yagin N, Pasdar Y, Nachvak SM, Abdollahzad H, et al. New insights on atherosclerosis: A cross-talk between endocannabinoid systems with gut microbiota. *J Cardiovasc Thorac Res*. 2018; 10: 129–37. <https://doi.org/10.15171/jcvtr.2018.21> PMID: 30386532
116. Ridlon JM, Kang DJ, Hylemon PB, Bajaj JS. Bile acids and the gut microbiome. *Curr Opin Gastroenterol*. 2014; 30: 332–8. <https://doi.org/10.1097/MOG.0000000000000057> PMID: 24625896
117. Wahlstrom A, Sayin SI, Marschall HU, Backhed F. Intestinal crosstalk between bile acids and microbiota and its impact on host metabolism. *Cell Metab*. 2016; 24: 41–50. <https://doi.org/10.1016/j.cmet.2016.05.005> PMID: 27320064
118. Fiorucci S, Biagioli M, Zampella A, Distrutti E. Bile acids activated receptors regulate innate immunity. *Front Immunol*. 2018; 9: 1853. <https://doi.org/10.3389/fimmu.2018.01853> PMID: 30150987
119. Nguyen TT, Ung TT, Kim NH, Jung YD. Role of bile acids in colon carcinogenesis. *World J Clin Cases*. 2018; 6: 577–88. <https://doi.org/10.12998/wjcc.v6.i13.577> PMID: 30430113
120. Tang W, Putluri V, Ambati CR, Dorsey TH, Putluri N, Amb S. Liver- and microbiome-derived bile acids accumulate in human breast tumors and inhibit growth and improve patient survival. *Clin Cancer Res*. 2019. <https://doi.org/10.1158/1078-0432.CCR-19-0094> PMID: 31296531
121. Magotti P, Bauer I, Igarashi M, Babagoli M, Marotta R, Piomelli D, et al. Structure of human N-acylphosphatidylethanolamine-hydrolyzing phospholipase D: regulation of fatty acid ethanolamide biosynthesis by bile acids. *Structure*. 2015; 23: 598–604. <https://doi.org/10.1016/j.str.2014.12.018> PMID: 25684574
122. Ritzhaupt A, Wood IS, Ellis A, Hosie KB, Shirazi-Beechey SP. Identification and characterization of a monocarboxylate transporter (MCT1) in pig and human colon: its potential to transport L-lactate as well as butyrate. *J Physiol*. 1998; 513 (Pt 3): 719–32.
123. Cohen MS, Chang P. Insights into the biogenesis, function, and regulation of ADP-ribosylation. *Nat Chem Biol*. 2018; 14: 236–43. <https://doi.org/10.1038/nchembio.2568> PMID: 29443986
124. Krukenberg KA, Kim S, Tan ES, Maliga Z, Mitchison TJ. Extracellular poly(ADP-ribose) is a pro-inflammatory signal for macrophages. *Chem Biol*. 2015; 22: 446–52. <https://doi.org/10.1016/j.chembiol.2015.03.007> PMID: 25865309
125. Ghani QP, Wagner S, Becker HD, Hunt TK, Hussain MZ. Regulatory role of lactate in wound repair. *Methods Enzymol*. 2004; 381: 565–75. [https://doi.org/10.1016/S0076-6879\(04\)81036-X](https://doi.org/10.1016/S0076-6879(04)81036-X) PMID: 15063698